

# Harnessing subspace controllability: Dynamical generation of Dicke states in Heisenberg-coupled qubit arrays with a single local control

Vladimir M. Stojanović,<sup>1</sup> Tommaso Calarco,<sup>2,3,4</sup> and Andrea Muratori<sup>2</sup>

<sup>1</sup>*Institut für Angewandte Physik, Technical University of Darmstadt, D-64289 Darmstadt, Germany*

<sup>2</sup>*Dipartimento di Fisica e Astronomia, Università di Bologna, 40127 Bologna, Italy*

<sup>3</sup>*Forschungszentrum Jülich GmbH, Peter Grünberg Institute,*

*Quantum Control (PGI-8), 52425 Jülich, Germany*

<sup>4</sup>*Institute for Theoretical Physics, University of Cologne, Zùlpicher Straße 77, 50937 Cologne, Germany*

(Dated: March 31, 2026)

We explore the feasibility of realizing Dicke states in qubit arrays with always-on isotropic Heisenberg coupling between adjacent qubits, assuming a single Zeeman-type control acting in the  $z$  direction on an actuator qubit. The Lie-algebraic criteria of controllability imply that such an array is not completely controllable, but satisfies the conditions for subspace controllability on any subspace with a fixed number of excitations. Therefore, a qubit array described by the model under consideration is state-to-state controllable for an arbitrary choice of initial and final states that have the same Hamming weight. This limited controllability is exploited here for the time-efficient dynamical generation of an  $a$ -excitation Dicke state  $|D_a^N\rangle$  ( $a = 1, 2, \dots, N - 1$ ) in a linear array with  $N$  qubits starting from a generic Hamming-weight- $a$  product state. To dynamically generate the desired Dicke states – including  $W$  states  $|W_N\rangle$  as their special ( $a = 1$ ) case – in the shortest possible time with a single local  $Z$  control, we employ an optimal-control scheme based on the *dressed Chopped Random Basis* (dCRAB) algorithm. We optimize the target-state fidelity over the expansion coefficients of smoothly-varying control fields in a truncated random Fourier basis; this is done by combining Nelder-Mead-type local optimizations with the multistart-based clustering algorithm that facilitates searches for global extrema. In this manner, we obtain the optimal control fields for Dicke-state preparation in arrays with up to 9 qubits. Based on our numerical results, we find that the shortest possible state-preparation times scale as  $\mathcal{O}(N^{2.08})$  for  $W$  states and  $\mathcal{O}(N^{1.78})$  for  $a = 2$  Dicke states. Finally, we demonstrate the robustness of our control scheme against small control-field distortions from the optimal pulse shape, as well as against control-field leakage away from the actuator qubit.

## I. INTRODUCTION

Introduced in the context of the phenomenon of super-radiance [1], Dicke states have in recent years been extensively investigated in connection with a variety of emerging quantum-technology applications. To be more specific, favorable properties of this class of highly-entangled multiqubit states [2] – above all, their extreme robustness to particle loss [3, 4], their immunity to collective dephasing noise [5], as well as their permutationally-symmetric character [6] – make them a viable candidate for applications in areas as diverse as quantum game theory [7], quantum networking [8], quantum metrology [9, 10], quantum error correction [11], and quantum combinatorial optimization [12], to name but a few.

Motivated by their anticipated promise in the realm of quantum technology, Dicke states have already been realized in several classes of physical systems. In addition, a multitude of proposals for the realization of those states in diverse physical systems were put forward in the past. Examples are furnished by trapped ions [13, 14], neutral atoms [15–18], spin-1/2 ensembles [19], photons [8, 20], and superconducting qubits [21]. It should be stressed, however, that most of the demonstrated schemes for the realization of Dicke states – as well as the existing theoretical proposals thereof – allow one to engineer only particular instances of those states, rather than an arbitrary state from this family [22]. Furthermore, most

of the envisioned state-preparation schemes are fraught with some additional limitations – for example, they require specific initial states (e.g. a Fock state), individual qubit addressing, or specific qubit-array topologies [23] as a prerequisite for realizing Dicke states.

In this paper, the feasibility of dynamical generation of Dicke states is investigated in the special case of linear qubit arrays with nearest-neighbor Heisenberg-type coupling and a single local control. This nontrivial quantum-state-engineering problem is addressed here by making use of the Lie-algebraic controllability criteria [24–27] and employing the optimal-control methods [28–31]. While the former guarantee the existence of time-dependent control fields that render the envisioned state-engineering scheme possible – but without specifying the actual time dependence of those fields – the latter can be utilized to determine the sought-after time dependence [32–34].

It is well-understood by now that the Heisenberg interaction between qubits by itself does not suffice for universal QC [35], by contrast to the Ising- and  $XY$ -type interactions [36]. It has been demonstrated, however, that universal QC can still be realized with the Heisenberg interaction alone if encoded qubit states – with the role of logical qubits being played by triples [35] or pairs [37] of physical qubits – are introduced, leading to the concept of encoded universality [38]. Another useful insight as to the potential relevance of this type of qubit-qubit coupling – which was also discussed in the context of

measurement-based QC [39] and stabilizer codes [40] – within the circuit model of QC came from Lie-algebraic studies of interacting spin-1/2 chains acted upon by time-dependent control fields [41, 42]. To be more specific, it was shown that a spin-1/2 chain with an “always-on” Heisenberg-type interaction [43] is completely controllable provided that at least two noncommuting controls – e.g., a Zeeman-type magnetic field with nonzero components in two mutually orthogonal directions (e.g.,  $x$  and  $y$ ) that act on a single spin (qubit) [42]. Under this last condition, an arbitrary (multiqubit) quantum gate can in principle be realized in such an array [44, 47, 48], which is equivalent to universal QC.

The fact that two local controls – that need not act on the same qubit [42] – are already sufficient for complete controllability of a Heisenberg-coupled  $N$ -qubit array begs the question whether an even smaller control resource – i.e., a single local control – permits some semblance of controllability in such an array. Indeed, it has already been shown that a single local control in such an array guarantees subspace controllability [46] on an arbitrary subspace of the total Hilbert space that is characterized by a fixed number  $a$  of excitations [42]. This also implies state-to-state controllability on each of those  $N + 1$  subspaces. In other words, for an arbitrary choice of initial- and final states with the same number of excitations (i.e. the same Hamming weight) it is possible to find control fields such that the total system dynamics – resulting from the interplay of the Heisenberg Hamiltonian and the control field – allows an evolution of the system from the given initial- to the desired final state.

The above Lie-algebraic results allow one to harness subspace controllability of Heisenberg-coupled qubit array with a single local control in the form of an analog (pulse-level) Dicke-state engineering scheme. Namely, given that the Dicke state with a certain excitation number  $a$  is the equal-weight linear combination of all possible product states with the same number of excitations, this Dicke state is reachable in the system at hand provided that one starts from a generic product state with the Hamming weight  $a$ . In other words, starting from an initial product state with  $a$  excitations at time  $t = 0$ , the  $a$ -excitation Dicke state can be dynamically generated at some later time  $t = T$ . To find the appropriate time-dependence of the control field that allows one to steer the system towards the desired Dicke state as rapidly as possible, i.e. in the shortest possible time  $T$ , the toolbox of quantum optimal control is employed here.

The control scheme utilized here for Dicke-state engineering relies on smoothly-varying control fields expanded over a truncated random Fourier basis of functions. The global maxima of the relevant figure of merit (target-state fidelity) as a function of the expansion coefficients of the control field are obtained by combining the Nelder-Mead simplex method for local optimization [50] and the multistart-based clustering algorithm that facilitates the search for global extrema [51]. In this manner, both the shortest possible times required for high-fidelity

realizations of Dicke and  $W$  states, as well as the corresponding optimal control fields, are obtained.

The remainder of this paper is structured as follows. To begin with, the definition and basic properties of Dicke states are reviewed in Sec. II. In Sec. III the main Lie-algebraic results pertaining to the controllability of spin-1/2 chains with nearest-neighbor Heisenberg-type coupling are recapitulated. The following, Sec. IV covers in detail the subspace controllability of the same class of systems. Section V specifies the system under investigation and the control objectives, as well as describing in detail the methodology for finding optimal control fields. The main findings of this work are presented and discussed in detail in Sec. VI. Finally, the paper is rounded out in Sec. VII, which also contains a brief summary of its principal findings.

## II. DICKE STATES: AN OVERVIEW

To set the stage for further considerations, the definition, basic properties, and concrete examples of Dicke states are provided below.

An  $a$ -excitation product state of an  $N$ -qubit system can be parameterized in the form  $|\{n_1, \dots, n_a\}\rangle$ , where  $n_1, \dots, n_a$  enumerate the qubits that are in the logical state  $|1\rangle$  and the remaining qubits are in the state  $|0\rangle$ . The  $N$ -qubit Dicke state with  $a$  excitations is given by the equal-weight superposition of all the product states  $|\{n_1, \dots, n_a\}\rangle$ , i.e.

$$|D_a^N\rangle = \binom{N}{a}^{-1/2} \sum_{n_1 < \dots < n_a}^N |\{n_1, \dots, n_a\}\rangle. \quad (1)$$

In other words, the  $N$ -qubit Dicke states with  $a$  excitations is the equal-weight linear combination of the  $\binom{N}{a}$  product states corresponding to the bit strings of Hamming weight  $a$ .

In the special, single-excitation ( $a = 1$ ) case Dicke states coincide with  $W$  states, i.e.  $|D_1^N\rangle \equiv |W_N\rangle$ , where

$$|W_N\rangle = \frac{1}{\sqrt{N}} (|10\dots 0\rangle + |010\dots 0\rangle + \dots + |0\dots 01\rangle) \quad (2)$$

is the  $N$ -qubit  $W$  state.  $W$  states constitute one of the most important classes of maximally-entangled multiqubit states and have many generalizations. Being more robust to particle loss than any other class of multiqubit states,  $W$  states hold promise for a multitude of quantum-technology applications; as a result, their realizations are proposed in all currently investigated physical platforms for QC [52–55].

Instead of the notation used in the above definition of Dicke states [cf. Eq. (1)], for small  $N$  it is more convenient to use a simpler notation that involves bit strings. For example, the two-excitation ( $a = 2$ ) Dicke state  $|D_2^3\rangle$  in a system of  $N = 3$  qubits, and its counterpart  $|D_2^4\rangle$  in

a 4-qubit system, are given by

$$\begin{aligned} |D_2^3\rangle &= \frac{1}{\sqrt{3}} (|110\rangle + |101\rangle + |011\rangle), \\ |D_2^4\rangle &= \frac{1}{\sqrt{6}} (|1100\rangle + |1010\rangle + |1001\rangle \\ &\quad + |0110\rangle + |0101\rangle + |0011\rangle). \end{aligned} \quad (3)$$

It is important to note that  $N$ -qubit Dicke states are invariant under arbitrary permutations of qubits. This property is manifest in yet another useful representation of Dicke states, equivalent to Eq. (1), which is given by

$$|D_a^N\rangle = \binom{N}{a}^{-1/2} \sum_{P \in S_N} P\{|1\rangle^{\otimes a} |0\rangle^{\otimes (N-a)}\}, \quad (4)$$

where the sum on the RHS of the last equation runs over all permutations  $P$  of the set  $\{1, 2, \dots, N\}$ , i.e. all elements of the symmetric group  $S_N$ . Moreover, Dicke states  $|D_a^N\rangle$  ( $a = 0, \dots, N-1$ ) form a basis of the permutationally-invariant subspace (the symmetric sector) of the  $2^N$ -dimensional  $N$ -qubit Hilbert space; the fact that this last subspace has the dimension  $N+1$ , which grows only linearly – rather than exponentially – with the number of qubits, explains its widespread use in quantum-information processing problems involving fully permutationally-invariant systems [56–61].

Another property of Dicke states that is of interest for the present work is that states  $|D_a^N\rangle$  and  $|D_{N-a}^N\rangle$  are equivalent up to local change of basis  $|0\rangle \rightleftharpoons |1\rangle$ ; therefore, these states have the same entanglement properties. In particular,  $W$  states  $|W_N\rangle \equiv |D_1^N\rangle$  and Dicke states  $|D_{N-1}^N\rangle$  are an example of such pairs of states.

### III. CONTROLLABILITY / REACHABILITY FOR HEISENBERG SPIN-1/2 CHAINS

In what follows, a survey of the principal Lie-algebraic results pertaining to Heisenberg-coupled qubit arrays is given, with emphasis on those of direct interest for the present work. The general Lie-algebraic framework of quantum control is first reviewed (Sec. III A). This is followed by a general introduction into the concept of local control (Sec. III B). Basic results pertaining to minimal control resources required for complete controllability of Heisenberg-coupled arrays are then discussed (Sec. III C).

Before embarking on discussions of general controllability and reachability criteria, as well as their applications to interacting spin-1/2 chains (qubit arrays), it is pertinent to introduce the notation that will be used in what follows for writing Hamiltonians of such systems. In particular, the single-qubit Pauli operators will be denoted by  $X$ ,  $Y$ , and  $Z$ ; using the standard computational basis, these operators can be expressed as  $X \equiv |0\rangle\langle 1| + |1\rangle\langle 0|$ ,  $Y \equiv i(|1\rangle\langle 0| - |0\rangle\langle 1|)$ , and  $Z \equiv |0\rangle\langle 0| - |1\rangle\langle 1|$ , while  $\mathbb{1}_2 = |0\rangle\langle 0| + |1\rangle\langle 1|$  is the single-qubit identity operator [36]. The counterparts of the operators  $X$ ,  $Y$ , and  $Z$  that act in the  $N$ -qubit Hilbert

space  $\mathcal{H} \equiv (\mathbb{C}^2)^{\otimes N}$  (the tensor product of single-qubit Hilbert spaces  $\mathbb{C}^2$ ) will be denoted by  $X_n$ ,  $Y_n$ , and  $Z_n$ , respectively, in the following. These last operators are jointly defined by the tensor-product relation

$$\mathbf{X}_n \equiv \mathbb{1}_2 \otimes \dots \otimes \mathbb{1}_2 \otimes \underbrace{\mathbf{X}}_n \otimes \mathbb{1}_2 \otimes \dots \otimes \mathbb{1}_2, \quad (5)$$

where  $\mathbf{X} \equiv (X, Y, Z)^T$  is the vector of single-qubit Pauli operators and  $\mathbf{X}_n \equiv (X_n, Y_n, Z_n)^T$  ( $n = 1, \dots, N$ ) that of their extension to the  $N$ -qubit Hilbert space.

#### A. Lie-algebraic controllability and reachability criteria for finite-dimensional quantum systems

Let us consider a quantum system, with the  $d$ -dimensional Hilbert space  $\mathcal{H}$ . Assume that  $H_0$  is the time-independent intrinsic (drift) Hamiltonian of this system and that the latter is acted upon by external control fields  $f_j(t)$  ( $j = 1, \dots, p$ ). These fields couple to certain degrees of freedom of the system, which are represented by Hermitian operators  $H_j$ . The total Hamiltonian of the system is then given by

$$H(t) = H_0 + \sum_{j=1}^p f_j(t) H_j. \quad (6)$$

The time-evolution operator  $U(t)$  of the system satisfies the time-dependent Schrödinger equation ( $\hbar = 1$ )

$$\frac{dU}{dt} = -i[H_0 + \sum_{j=1}^p f_j(t) H_j] U(t), \quad (7)$$

with the initial condition  $U(t=0) = \mathbb{1}_d$ , where  $\mathbb{1}_d$  is the identity operator on the Hilbert space  $\mathcal{H}$  [27]. The objective of a generic quantum-control problem is to determine a time  $T > 0$  and time-dependent controls  $f_j(t) \in \mathbb{R}$  such that a desired unitary  $U_{\text{target}}$  is reached at  $t = T$ ; in other words,  $U(t=T) = U_{\text{target}}$ . In particular, the system is said to be completely (operator) controllable provided that its dynamics, governed by  $H(t)$ , gives rise – with a certain choice of the fields  $f_j(t)$  – to an arbitrary unitary on its Hilbert space. Rephrasing, complete controllability assumes that the reachable set of the system – i.e., the set of unitaries achievable by varying the controls – is given by the Lie group  $U(d)$  or  $SU(d)$  [27].

The criteria of controllability for quantum systems are framed using Lie-algebraic concepts [24–27], among which that of the dynamical Lie algebra (DLA) of the system plays the principal role [27]. For a system governed by the Hamiltonian in Eq. (6), the DLA  $\mathcal{L}$  is generated by the skew-Hermitian counterparts of the operators  $H_k$ . i.e. by the operators  $\{-iH_k | k = 0, \dots, p\}$ . The necessary and sufficient condition for complete controllability (the Lie-algebraic rank condition) [27] is that  $\mathcal{L}$  be isomorphic to the Lie algebra  $u(d)$  of skew-Hermitian  $d \times d$  matrices, or its counterpart  $su(d)$  that corresponds to traceless skew-Hermitian ones [62]. This general result constitutes an existence theorem that guarantees that any

unitary on the Hilbert space of the system is reachable for appropriately chosen control fields. Another, completely separate, question is how to find the actual time dependence of control fields that allows one to realize a desired unitary. This is typically done by taking into account various additional constraints – most prominently, the one pertaining to the total duration of the control protocol.

### B. Local (quantum) control: general concept and its application to qubit arrays

The principal control-related issue pertaining to interacting quantum systems is whether a given system can be fully- or, at least, partially controlled by solely acting on its subsystem. This is the idea of the *local-control* approach, which assumes that only a small subsystem of the original system is subject to control fields. The actual choice of the subsystem crucially depends on the type of interaction in the considered quantum system.

Let us consider a composite system  $S = C \cup \bar{C}$ , described by the Hamiltonian

$$H(t) = H_S + \sum_j f_j^C(t) H_j^C, \quad (8)$$

where  $H_S$  is the drift part (acting on the whole system  $S$ ), while  $H_j^C$  are local Hamiltonians (acting only on the subsystem  $C$ ) and  $f_j^C(t)$  the corresponding time-dependent control fields (for an illustration, see Fig. 1). Assuming, for simplicity, that  $-iH_j^C$ 's generate the Lie algebra  $\mathcal{L}(C)$  on  $C$ , the system  $S$  is completely controllable iff  $-iH_S$  and  $-iH_j^C$  generate  $\mathcal{L}(S)$ , i.e.,

$$\langle iH_S, \mathcal{L}(C) \rangle = \mathcal{L}(S), \quad (9)$$

where  $\langle A, B \rangle$  stands for the algebraic closure of the operator sets  $A$  and  $B$  [62]. Therefore, any unitary on  $S$  can be enacted through control of its subsystem  $C$  iff every element of  $\mathcal{L}(S)$  can be obtained either as linear combinations of  $-iH_S$ ,  $-iH_j^C$ , or their repeated commutators.

Qubit arrays constitute a prototypical class of systems in which local-control approach may be advantageous [63]. In keeping with the above Lie-algebraic criteria (cf. Sec. III A), complete controllability of an  $N$ -qubit array is that its corresponding DLA be isomorphic with either  $u(2^N)$  or  $su(2^N)$ . The conventional approach to control in a qubit array requires control fields to act on each qubit in the array. Along with a drift Hamiltonian, which describes qubit-qubit interactions that make it possible to realize entangling two-qubit gates, this – in principle – permits the realization of an arbitrary (multi-qubit) gate. In contrast to this scenario, in the local-control case control fields act only on a handful of *actuator* qubits – in the extreme case, a single qubit. The specific choice of actuator qubits in a given system should ideally be one guaranteeing complete controllability, as the latter renders universal QC possible [27].

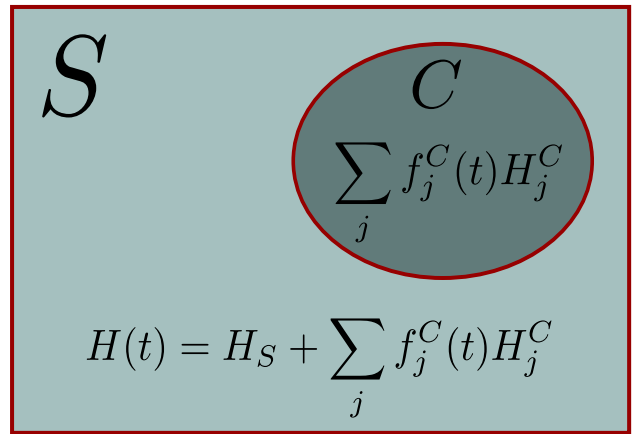


FIG. 1: Pictorial illustration of the concept of local control. System  $S$  is described by the drift Hamiltonian  $H_S$ . The system is subject to external control fields  $f_j^C(t)$ , which couple only to its degrees of freedom that belong to the subsystem  $C$ ; these degrees of freedom are described by the local Hamiltonians  $H_j^C$ . The total Hamiltonian of the system is then the one given by Eq. (8).

The usefulness of local control in qubit arrays cannot be overstated, especially in the context of solid-state qubits. In principle, global-control approaches to qubit arrays constitute a promising pathway to scalable QC [64]. In particular, a continuous-wave global field permits decoupling of the qubits from background noise. In the case of solid-state qubits this approach is, however, compromised by the unavoidable variability in the parameters of individual qubits in the array (e.g. statistical scatter in qubit resonance frequency). Therefore, applications of global-control strategies in solid-state QC platforms usually require additional nontrivial contingencies [65–67], especially in large-scale systems [68].

### C. Complete controllability of Heisenberg-coupled spin-1/2 chains (qubit arrays): principal results

The issue of identifying the minimal control resources required for complete controllability of various interacting spin-1/2 models (Ising,  $XY$ , Heisenberg, etc.) was studied extensively in the past [41, 42]. For each of these models, the smallest subsystem was sought that – when acted upon by Zeeman-type external controls – renders the entire chain completely controllable. As it turned out, only for Heisenberg-type coupling these investigations yielded nontrivial results.

The most general controllability-related result for spin-1/2 chains (qubit arrays) with Heisenberg-type interaction was proven based on a method that makes use of the Hilbert-space decomposition into a tensor product of minimal invariant subspaces [42]. This result asserts that the existence of two mutually noncommuting local controls – which need not act on the same spin (qubit) – guarantees complete controllability of the chain;

importantly, this last result holds even when for fully anisotropic  $XYZ$  coupling case [42], i.e., for the drift Hamiltonian

$$H_{XYZ} = \sum_{n=1}^{N-1} (J_x X_n X_{n+1} + J_y Y_n Y_{n+1} + J_z Z_n Z_{n+1}), \quad (10)$$

where  $J_x$ ,  $J_y$ , and  $J_z$  are the three coupling strengths. While the last controllability-related result does not require the two noncommuting controls to act on the same qubit, the simplest scenario to which this theorem applies is the one in which the first qubit in the array is subject to a Zeeman-type field control field  $\mathbf{B}_1(t)$  with two nonzero components. Assuming, for definiteness, that these components are  $x$  and  $y$ , i.e. that  $\mathbf{B}_1(t) \equiv [B_{1x}(t), B_{1y}(t), 0]^T$ , the corresponding control Hamiltonian is given by

$$H_c(t) = B_{1x}(t)X_1 + B_{1y}(t)Y_1. \quad (11)$$

The stated general controllability result, pertaining to the drift Hamiltonian  $H_{XYZ}$  [cf. Eq. 10], has two special cases that had been proven long before the general one. The first of these special cases is that of the  $XXZ$  drift Hamiltonian

$$H_{XXZ} = J \sum_{n=1}^{N-1} (X_n X_{n+1} + Y_n Y_{n+1} + \Delta Z_n Z_{n+1}), \quad (12)$$

where  $J_x = J_y \equiv J$  and  $J_z \equiv J\Delta$ , with  $\Delta$  being the anisotropy parameter. The second special case corresponds to the fully isotropic Heisenberg Hamiltonian (i.e. the one with  $J_x = J_y = J_z \equiv J$ )

$$H_{XXX} = J \sum_{n=1}^{N-1} (X_n X_{n+1} + Y_n Y_{n+1} + Z_n Z_{n+1}), \quad (13)$$

which happens to be of most relevance for applications in realistic qubit arrays [66].

Two extreme scenarios that permit complete controllability of Heisenberg-coupled qubit arrays are illustrated in Fig. 2. An example of a qubit array with the fully anisotropic Heisenberg interaction [cf. Eq. (10)] and two noncommuting local Zeeman-type controls applied to different qubits – more precisely, one interior qubit (qubit 2) and one of the end qubits (qubit  $N$ ) – is shown Fig. 2(a). On the other hand, an example of a qubit array with the isotropic Heisenberg interaction [cf. Eq. (13)] and two noncommuting local Zeeman-type controls, both applied to same end qubit (qubit 1) is depicted in Fig. 2(b).

For each of the Hamiltonians in Eqs. (10)-(13), complete controllability of the underlying system can be proven by demonstrating that its corresponding DLA, generated by the skew-Hermitian counterparts of the drift Hamiltonian [i.e.,  $-iH_{XYZ}$ ,  $-iH_{XXZ}$ ,  $-iH_{XXX}$ , for the drift Hamiltonians in Eqs. (10)-(13), respectively] and the two single-spin(qubit) Pauli operators describing noncommuting controls [e.g.,  $-iX_1$  and  $-iY_1$  in the

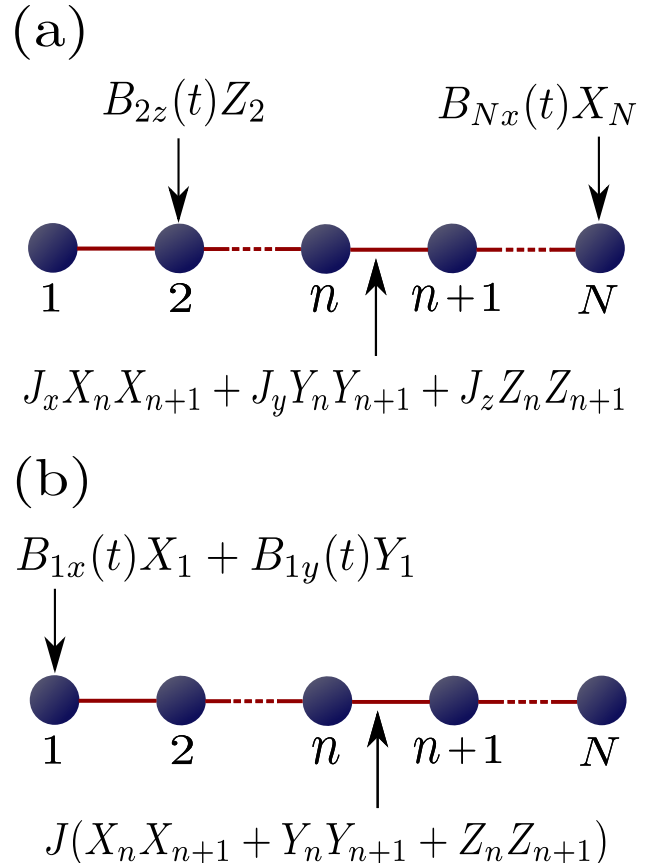


FIG. 2: Schematic illustration of possible complete-controllability scenarios in Heisenberg-coupled  $N$ -qubit arrays with a local control: (a) In an array with the fully anisotropic Heisenberg interaction a local  $Z$  control is applied to qubit 2 and local  $X$  control to qubit  $N$ , (b) In an array with the isotropic Heisenberg interaction local  $X$ - and  $Y$  controls are both applied to qubit 1.

example of the control Hamiltonian in Eq. (11)], has the dimension equal to  $d^2 - 1$  (note that each of the above drift Hamiltonians, as well as the control Pauli operators, is traceless) with  $d \equiv 2^N$  being the dimension of the Hilbert space of the system. This implies that the relevant DLA is isomorphic with the Lie algebra  $su(d)$  [62].

#### IV. SUBSPACE CONTROLLABILITY OF HEISENBERG SPIN-1/2 CHAINS

The crucial control-related concept for the remainder of this work, providing the theoretical underpinning for the optimal-control-based generation of Dicke states, is that of subspace controllability. General aspects of this concept are discussed in Sec. IV A below. The discussion in Sec. IV B specializes to subspace controllability of  $XXZ$ - and  $XYZ$ -type Heisenberg spin-1/2 chains.

### A. Subspace controllability: general aspects

Among different situations that can be encountered when discussing controllability of finite-dimensional quantum systems, subspace controllability refers to the one in which the underlying Hilbert space can be split into the direct sum of invariant subspaces and, on each of these invariant subspaces, it is possible to generate any arbitrary unitary operation using appropriately chosen control functions [42]; this also implies state-to-state controllability for any choice of initial- and final states that belong to this same subspace.

Familiar examples of subspace controllability are furnished by permutationally-symmetric networks of qubits [69] – e.g., that of all-to-all Ising( $zz$ )-coupled qubits subject to transverse ( $x$  and  $y$ ) global control fields [6, 56, 70–72], where the relevant subspace is the  $(N + 1)$ -dimensional permutationally-invariant subspace (symmetric sector) of the total  $N$ -qubit Hilbert space (cf. Sec. II) [73]. Another example is that of  $XY$ -coupled spin-1/2 chain (qubit array) with a single local control [cf. Sec. IV B below], where subspace controllability holds only for the single-excitation subspace [42].

The existence of controllable subspaces is a common situation in cases where the system under consideration possesses dynamical symmetries [45, 46]. In the context of quantum control of a general quantum system [recall Sec. III A], with the drift Hamiltonian  $H_0$  and  $p$  external controls described by Hamiltonians  $H_j$  ( $j = 1, \dots, p$ ), any Hermitian operator  $S$  that is not a multiple of the identity and commutes with both  $H_0$  and all  $H_j$  ( $j = 1, \dots, p$ ), i.e. satisfies the condition  $[H_0, S] = [H_j, S] = 0$ , is referred to as the symmetry operator of the system. It follows directly that the operators  $H_0$ ,  $H_j$  ( $j = 1, \dots, p$ ), and  $S$  can be simultaneously diagonalized.

### B. Subspace controllability of $XXZ$ - and $XYZ$ -type Heisenberg-coupled spin-1/2 chains

The existing studies of subspace controllability of Heisenberg-coupled spin-1/2 chains showed that for this class of models subspace controllability depends on whether the (two-local) interactions in the two directions perpendicular to the control direction are equal or not, i.e., whether the spin-1/2 chain is of  $XXZ$  type – including the fully isotropic  $XXX$  case – or anisotropic  $XYZ$  type [42]. Due to the significantly higher degree of symmetry in the  $XXZ$  case, the character of dynamical symmetries – accordingly, that of invariant subspaces as well – is different in these two cases.

In the case of  $XXZ$ -type Hamiltonians [cf. Eq. (12)] – including the special case  $\Delta = 1$  [i.e. the isotropic ( $XXX$ ) Heisenberg Hamiltonian in Eq. (13)] – it is per-

tinuous to introduce the excitation operator

$$S_{\text{exc}} = \frac{1}{2} \sum_{n=1}^N (\mathbb{1}_2 + Z_n). \quad (14)$$

It is worthwhile noting that this operator can be recast as  $S_{\text{exc}} = S_z + N/2$ , where

$$S_z = \frac{1}{2} \sum_{n=1}^N Z_n \quad (15)$$

is the  $z$  projection of the collective-spin operator of the system. The excitation operator has  $N + 1$  distinct eigenvalues  $a = 0, 1, \dots, N$ . Therefore, the Hilbert space of the system can be decomposed as a direct sum of its eigensubspaces, i.e.  $\mathcal{H} = \bigoplus_{a=0}^N \mathcal{H}_a$ . In particular, the eigensubspace  $\mathcal{H}_a$  is generated by the states corresponding to bit-strings with exactly  $a$  occurrences of 1, i.e.  $a$ -excitation states (also known as Hamming-weight- $a$  states).

It is straightforward to verify that  $[H_{XXZ}, S_{\text{exc}}] = 0$ . Provided that the relevant control Hamiltonians  $H_j$  contain only Pauli- $Z$  operators, then  $S_{\text{exc}}$  commutes with all of them and defines a symmetry, which is referred to as the excitation symmetry. As a result, both the Hamiltonian  $H_{XXZ}$  and control Hamiltonians can be block-diagonalized on each of the  $N + 1$  eigensubspaces  $\mathcal{H}_a$  of  $\mathcal{H}$ , which in that case also represent the invariant subspaces of the system. It is straightforward to see that for an  $N$ -qubit system, the dimension of  $\mathcal{H}_a$  is given by

$$\dim \mathcal{H}_a = \binom{N}{a} = \frac{N!}{a!(N-a)!}. \quad (16)$$

In particular, the largest of these invariant subspaces is the one that for  $N$  even corresponds to  $a = N/2$  (in the case of odd  $N$  it corresponds to  $a = \lfloor N/2 \rfloor$ ); the asymptotic dimension of this subspace for large  $N$  grows exponentially with  $N$  [74]; namely, by making use of the Stirling formula  $N! \approx \sqrt{2\pi N} (N/e)^N$  (for large  $N$ ) one finds that  $\dim \mathcal{H}_{N/2} \sim 2^N / \sqrt{\pi/2N}$  for large  $N$ .

As already proven in [42], an  $XXZ$  spin-1/2 chain of length  $N$  with a single local  $Z$  control on an end spin is controllable on each of the  $N + 1$  invariant excitation subspaces  $\mathcal{H}_0, \dots, \mathcal{H}_N$ . It is important to stress that this last result also holds for the special case of an isotropic Heisenberg  $XXX$  chain. However, in the latter case, owing to the absence of preferred spatial direction (i.e. the symmetry between the  $x$ ,  $y$ , and  $z$  directions), this result applies for a local control in any of the three directions.

Two possible subspace-controllability scenarios in spin-1/2 chains (qubit arrays) with  $XXZ$ -type Heisenberg interaction are illustrated in Fig. 3. While Fig. 3(a) depicts the most general  $XXZ$ -interaction case – where a single local control ought to be applied in the  $z$  direction – Fig. 3(b) illustrates the special case of isotropic Heisenberg interaction, where a control in the  $x$  direction is equally permissible as one in the  $z$  direction.

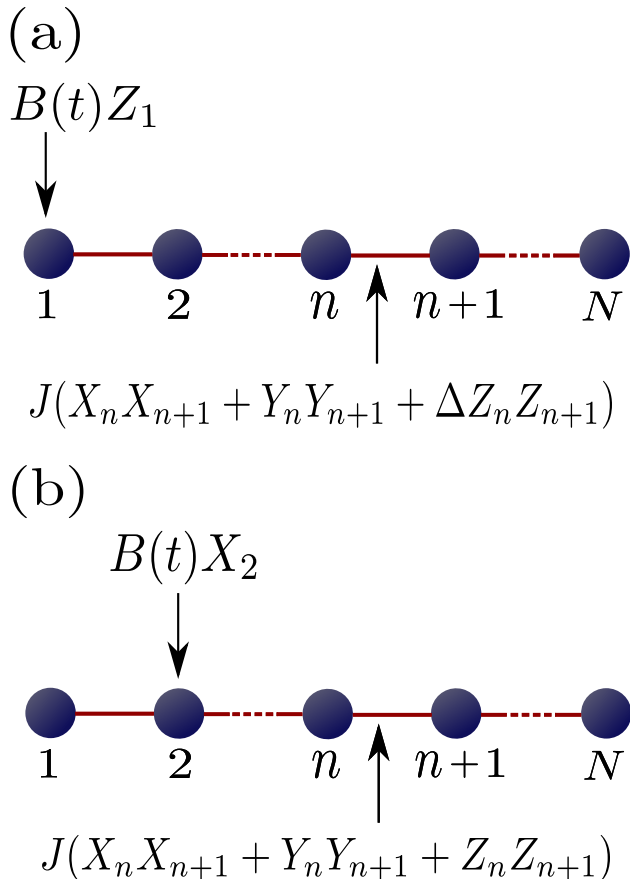


FIG. 3: Schematic illustration of possible subspace-controllability scenarios in Heisenberg-coupled  $N$ -qubit arrays with a local control effected through a unidirectional time-dependent magnetic field of magnitude  $B(t)$ : (a) In an array with the  $XXZ$ -type Heisenberg interaction a local  $Z$  control is applied to qubit 1, (b) In an array with the isotropic Heisenberg interaction a local  $X$  control is applied to qubit 2.

By contrast to the  $XXZ$  case, for the  $XYZ$  model [cf. Eq. (10)] the excitation symmetry [represented by the operator  $S_{\text{exc}}$  in Eq. (14)] – is not one of the dynamical symmetries. However, this model does have the  $Z$ -parity symmetry, represented by the operator  $S_P = Z_1 Z_2 \dots Z_N$ ;  $H_{XYZ}$  has two  $2^{N-1}$ -dimensional invariant subspaces  $\mathcal{H}_1$  and  $\mathcal{H}_{-1}$ , which correspond to the eigenvalues  $\pm 1$  of  $S_P$ , respectively. Therefore, compared to the  $XXZ$  case, the number of invariant subspaces in the  $XYZ$  chain is reduced from  $N + 1$  to 2 as a consequence of symmetry breaking between the  $x$  and  $y$  directions. Similarly to the  $XXZ$  case, it was proven that an  $XYZ$  spin-1/2 chain of length  $N$  with a single local  $Z$  control on an end spin, the system is indeed controllable on each of the two invariant subspaces  $\mathcal{H}_1$  and  $\mathcal{H}_{-1}$  [42].

For the sake of completeness, it is worthwhile mentioning that in the absence of the  $ZZ$  coupling [i.e. in the special case  $J_z = 0$  of Eq. (10)] – i.e. for the  $XY$ -type Hamiltonians (including its special case  $J_x = J_y \equiv J$ , known as the  $XX$  Hamiltonian) – the subspace controllability

holds only in the single-excitation subspace ( $a = 1$ ). It is also useful to mention that an interesting class of highly-entangled multiqubit states that belong to such a subspace is that of  $W$ -type (Hamming-weight-1) states; the most important subclass of such states are the conventional, maximally-entangled  $W$  states [cf. Eq. (2)].

Without significant loss of generality, the analysis of the dynamical generation of Dicke states in the remainder of this work (see Secs. V and VI below) will be carried out only in the isotropic Heisenberg-interaction case, described by the Hamiltonian  $H_{XXX}$ . This choice is primarily motivated by the practical relevance of isotropic Heisenberg interactions in realistic qubit arrays, e.g. those based on spin qubits [66].

## V. DYNAMICAL GENERATION OF DICKE STATES WITH A LOCAL CONTROL

The subspace-controllability results reviewed in Sec. IV B are utilized in the following for the dynamical generation of Dicke states in qubit arrays with the isotropic Heisenberg interaction between adjacent qubits. The connection between these subspace-controllability results and the reachability of Dicke states is explained in Sec. V A below, where the Dicke-state generation is also framed as a quantum-control problem. In Sec. V B, various approaches to quantum optimal control are briefly surveyed, with emphasis on their potential advantages for solving this last problem. Finally, the dCRAB algorithm – our method of choice for designing optimal control fields in the problem at hand – is then briefly described in Sec. V C.

### A. Generation of $|D_a^N\rangle$ in qubit arrays with isotropic Heisenberg-type interaction

As already expounded in Sec. IV B, an array of  $N$  qubits with nearest-neighbor isotropic Heisenberg interaction and a single local control acting in  $x$ ,  $y$ , or  $z$  direction satisfy the criteria for subspace controllability on any subspace  $\mathcal{H}_a$  with the fixed number  $a$  of excitations ( $a = 1, 2, \dots, N - 1$ ). All such qubit arrays are described by time-dependent Hamiltonians of the form

$$H(t) = J \sum_{n=1}^{N-1} (X_n X_{n+1} + Y_n Y_{n+1} + Z_n Z_{n+1}) + \mathbf{B}(t) \cdot \mathbf{X}_{n_c}. \quad (17)$$

where  $\mathbf{B}(t)$  stands for the unidirectional external Zeeman-type control field and  $\mathbf{X}_{n_c} \equiv (X_{n_c}, Y_{n_c}, Z_{n_c})$  is the vector of Pauli operators [cf. Sec. III] corresponding to the actuator qubit  $n = n_c$ . For instance,  $\mathbf{B}(t) = [0, 0, B(t)]$  and  $n_c = 1$  correspond to the situation where qubit 1 is acted upon by a local Pauli- $Z$  control; similarly,  $\mathbf{B}(t) = [B(t), 0, 0]$  and  $n_c = 2$  if qubit 2 is acted upon by a Pauli- $X$  control.

One immediate implication of the subspace controllability of qubit arrays described by the Hamiltonians in Eq. (17) is the state-to-state controllability of such a system on each of the  $N + 1$  subspaces; therefore, for an initial  $N$ -qubit state with a certain number  $a$  of excitations, any other  $N$ -qubit state with the same number of excitations (i.e. the same Hamming weight) is reachable – through an appropriately chosen time-dependent control field – in this system.

The established reachability of an arbitrary  $N$ -qubit state with a fixed number  $a$  of excitations – from any other state with the same number of excitations – can be harnessed for the purpose of engineering Dicke states in the system under consideration. The  $N$ -qubit Dicke state  $|D_a^N\rangle$  with  $a$  excitations ( $a = 1, 2, \dots, N - 1$ ), the equal-weight linear combination of all possible product states with the same number of excitations [cf. Eqs. (1) and (4)], is reachable in the system at hand provided that one starts from a generic product state with the Hamming weight  $a$ ; all such product states can succinctly be written in the form  $P\{|1\rangle^{\otimes a}|0\rangle^{\otimes(N-a)}\}$ , where  $P$  is an arbitrary permutation of the set  $\{1, 2, \dots, N\}$ . Therefore, if one starts from, e.g., the initial state

$$|\psi(t=0)\rangle = |1\rangle^{\otimes a}|0\rangle^{\otimes(N-a)} \equiv \underbrace{|11\dots 1\rangle}_a \underbrace{|00\dots 0\rangle}_{N-a}, \quad (18)$$

then the above Lie-algebraic result guarantees that an appropriate time dependence of the field  $B(t)$  can be found such that at a later time  $T$  the Dicke state  $|D_a^N\rangle$  of the  $N$ -qubit array is engineered, i.e.

$$|\psi(t=T)\rangle = |D_a^N\rangle. \quad (19)$$

In this manner, the state  $|D_a^N\rangle$  is dynamically generated within a time interval of duration  $T$  from an initial Hamming-weight- $a$  product state [cf. Eq. (18)].

While, as explained above, the subspace controllability of the system holds for each of the three possible directions of  $\mathbf{B}(t)$  [cf. Sec. IV B], Dicke states are eigenstates of the  $z$  projection  $S_z$  of the collective spin operator [cf. Eq. (15)], where the eigenvalue corresponding to the state  $|D_a^N\rangle$  is given by  $N/2 - a$ . This is what makes the  $z$  direction special as far as Dicke states are concerned. Because of that, we will discuss dynamical generation of Dicke states with a local  $Z$  control on the first qubit (for an illustration, see Fig. 4), which constitutes one special realization of the family of the local-control Hamiltonians in Eq. (17). Therefore, the control part of the total system Hamiltonian will hereafter have the form  $B(t)Z_1$ . The total Hamiltonian of an  $N$ -qubit array under such circumstances is then given by

$$H(t) = J \sum_{n=1}^{N-1} (X_n X_{n+1} + Y_n Y_{n+1} + Z_n Z_{n+1}) + B(t)Z_1. \quad (20)$$

The dynamical generation of Dicke states in a qubit array described by the Hamiltonian of Eq. (20), with the

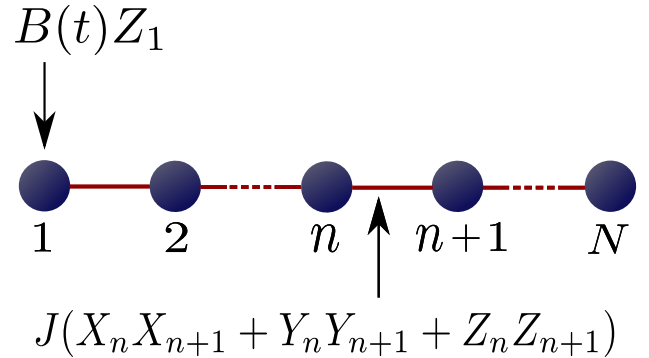


FIG. 4: Schematic illustration of an  $N$ -qubit array with nearest-neighbor isotropic Heisenberg interaction and a local  $Z$  control acting on the first qubit in the array.

first qubit playing the role of actuator [i.e.  $n_c = 1$  in Eq. (17)], is investigated in what follows. Our main control objective in the following is to find the shortest possible ( $N$  and  $a$ -dependent) evolution time  $T = T_{\min}$  that allows one to realize the desired Dicke state  $|D_a^N\rangle$ , as well as the corresponding (state-specific) time dependence of the control field  $B(t)$ . The control-field magnitude in the problem at hand will be expressed in units of the coupling strength  $J$ ; at the same time, all the relevant times will be expressed in units of  $J^{-1}$  (recall that  $\hbar = 1$ ).

Needless to say, the appropriate time-dependence  $B(t)$  of the control field that allows one to engineer the desired Dicke state  $|D_a^N\rangle$  within the shortest possible time  $T = T_{\min}$  – and this minimal time itself – do not follow from the above Lie-algebraic results on subspace controllability of Heisenberg-coupled qubit arrays, but ought to be determined by altogether different means. To this end, we employ advanced methods of quantum optimal control (for details, see Secs. V B and V C below).

The Dicke-state generation problem under consideration is that of engineering a target state of a closed quantum system – up to an unimportant global phase – in a finite time  $T$ . Therefore, the relevant figure of merit in this problem is the target-state fidelity

$$\mathcal{F}_{t=T} = |\langle \psi(t=T) | D_a^N \rangle|^2, \quad (21)$$

i.e. the module squared of the overlap between the actual state  $|\psi(t=T)\rangle$  of the system at time  $t=T$  and the target Dicke state  $|D_a^N\rangle$ ; the state  $|\psi(t=T)\rangle$  is given by  $U(t=T)|\psi(t=0)\rangle$ , where  $U(t)$  is the time-evolution operator of the system, i.e. the one corresponding to the Hamiltonian in Eq. (20) [for details of the numerical evaluation of  $U(t)$ , see Sec. (V B) below]. For each sought-after Dicke state (i.e. for each different choice of  $N$  and  $a$ ), the aim is to find the time dependence  $B(t)$  of the control field that maximizes the state fidelity.

## B. Quantum optimal-control schemes

In the following, we describe the optimal-control approach to be employed in what follows for finding the time dependence  $B(t)$  of the control field that permits the realization of the desired Dicke states in an array with  $N$  qubits.

It is a common practice in quantum optimal control to start with piecewise-constant control fields [75]. In that case the time-evolution operator  $U(t)$  of the system – describing its dynamics for  $0 \leq t \leq T \equiv N_f \Delta t$  – is given by a product of factors of the form  $\exp[-i(H_0 + H_C^{(k)})\Delta t]$ , which is characteristic of time-independent Hamiltonians; here  $H_0$  is the drift Hamiltonian of the system and  $H_C^{(k)}$  the (time-independent) control Hamiltonian during the  $k$ -th time interval of duration  $\Delta t$  ( $k = 1, \dots, N_f$ ) in which the control field has a constant value  $B_k$ .

Among the quantum optimal-control schemes that rely on piecewise-constant control fields, the most widely used one is based on the GRAdient Ascent Pulse Engineering (GRAPE) algorithm [76]. The latter iteratively updates the control-field values in each piecewise-constant step in order to maximize the relevant figure of merit. Other notable numerical method that employs piecewise-constant control fields is the Krotov algorithm [77], distinguished by its enhanced convergence properties. Similar to GRAPE, the Krotov algorithm belongs to the group of gradient-based, open-loop optimization methods. Finally, it is worthwhile to mention the recently proposed GEODESIC Pulse Engineering (GEOPE) [81], which relies on differential programming and geodesics on the Riemannian manifold of  $SU(2^N)$ .

While working with piecewise-constant control fields has certain advantages, in this work we make use of smooth time-dependent control pulses. By contrast to the piecewise-constant case, in this continuous-wave approach to quantum optimal control the total system Hamiltonian  $H(t)$  carries an explicit time dependence and, in general, does not commute with itself at different times, i.e.  $[H(t'), H(t'')] \neq 0$ . Consequently, the time-evolution operator of the system is given by the most general form, which entails a time-ordered exponential:

$$U(t) = \mathcal{T} \exp \left[ -i \int_0^t H(t') dt' \right]. \quad (22)$$

Therefore, for a finite-time dynamical evolution of the system, such time-evolution operator ought to be determined by purely numerical means.

In addition to gradient-based algorithms for optimal control, there are also approaches that are not gradient-based and incorporate bandwidth limitation and smooth pulses in a few-parameter Ansatz. Examples of such approaches are furnished by the CRAB (Chopped RANdom Basis) formalism [78], which encodes pulses in a chopped randomized Fourier basis, as well as its improvement called dressed-CRAB (dCRAB) [79] (see the detailed description in Sec. VC below); another exam-

ple for optimal-control algorithms of this class is GRAFS (GRAdient Ascent in Function Space) [80], which places special emphasis on smooth control fields. Motivated by its superior convergence properties, enhanced compared to its parent CRAB algorithm, in the state-engineering problem at hand we employ the dCRAB algorithm [79].

## C. dCRAB: a short description of the algorithm

In what follows, we describe the essential ingredients of the dCRAB algorithm [79], along with some basic features of our own implementation thereof in the problem under consideration. These features include, e.g., our approach to global optimization – which is more advanced than the one conventionally used in applications of the dCRAB formalism – as well as some quantitative implementation-related details (e.g., the chosen threshold value of the figure of merit in the problem at hand).

The first issue in any application of the dCRAB formalism is the choice of the functional basis in which to parametrize the control fields. While, in principle, different bases can be employed in conjunction with the dCRAB formalism, we parametrize our smooth control pulses using a truncated randomized Fourier basis, i.e. a basis that consists of a finite number of sine- and cosine harmonics with randomly sampled frequencies. In this basis, the control field  $B(t)$  is decomposed as

$$B(t) = \sum_{m=0}^{M-1} [c_m \cos(\omega_m t) + s_m \sin(\omega_m t)], \quad (23)$$

where  $\omega_m$  are randomly chosen frequencies within a given interval; here, we take  $\omega_m = 2\pi(m + r_m)/T$ , where  $r_m$  is randomly sampled in the interval  $[-0.5, 0.5]$  and  $T$  denotes the total evolution time. As a consequence of the dependence of the control field  $B(t)$  on the parameters  $\{c_0, c_1, \dots, c_{M-1}\}$  and  $\{s_0, s_1, \dots, s_{M-1}\}$ , the time-evolution operator  $U(t)$  of the system is also a function of those parameters. By extension, the same is true of the state  $|\psi(t=T)\rangle$  of the system at  $t=T$  and the target-state infidelity  $1 - \mathcal{F}_{t=T}$  [cf. Eq. (21)]. While the steps described up to now constitute the standard CRAB optimization, it is worthwhile taking into account that the basis has a finite number of degrees of freedom and the convergence may end in a non-optimal fixed point. The principal idea of dCRAB is then to dress the obtained pulse with new iterations of CRAB, namely by introducing a new pulse

$$B^{(l)}(t) = B^{(l-1)}(t) + \sum_{m=0}^{M-1} [c_m^{(l)} \cos(\omega_m^{(l)} t) + s_m^{(l)} \sin(\omega_m^{(l)} t)], \quad (24)$$

where  $\omega_m^{(l)}$  are newly sampled random frequencies,  $B^{(l-1)}(t)$  denotes the pulse obtained at the previous

CRAB iteration, and  $l$  enumerates repetitions of the dressing procedure. The optimization is performed once again, using  $\{c_m^{(l)}, s_m^{(l)}\}$  as optimization parameters and keeping  $B^{(l-1)}(t)$  fixed. The complete functional form of the pulse in the end reads

$$B(t) = \sum_{l=0}^{L-1} \sum_{m=0}^{M-1} \left[ c_m^{(l)} \cos(\omega_m^{(l)} t) + s_m^{(l)} \sin(\omega_m^{(l)} t) \right], \quad (25)$$

where  $L$  denotes the total number of dressing iterations. Here, we set a maximum value of  $L_{\max} = 10$ , with the possibility of an early termination of the dressing procedure (hence, of the whole optimization as well) if the figure of merit is below a chosen threshold value (here  $1 - \mathcal{F}_{t=T} = 10^{-3}$ ). We recall once again that, in the pulse parametrization of Eq. (25), the optimization parameters  $\{c_m^{(l)}, s_m^{(l)}\}$  are not optimized all at once, but for one value of  $l$  at a time.

We carry out local searches for the minima of the target-state infidelity  $1 - \mathcal{F}_{t=T}$  [cf. Eq. (21)] using the Nelder-Mead simplex method [50]. Moreover, to account for the complexity of the optimization landscape in the problem at hand, we also make use of the *multistart-based clustering* (also known as *multistart-based global random search*) algorithm [51]. The latter is widely used for finding global minima of objective functions that have a large number of very close local minima [82, 83] and consists of the following steps. Firstly, one randomly selects a large ( $\sim 10^3$ ) sample of points in the candidate-solution space. Secondly, one selects a much smaller ( $\sim 20$ ) number of points that yield the smallest values of the objective function (in the case at hand, the target-state infidelity) and performs local searches for minima around each of them; the one with the smallest value of the objective function is then adopted as the desired global minimum. The adequacy of this algorithm is corroborated by the stability of the obtained result for the global minimum of the objective function upon altering the number of random points in the initial step of the algorithm. Here, this strategy is used at the beginning of each dressing iteration, to obtain the best initial sample for global minimization.

The whole procedure described above allows the encoding of limited-bandwidth pulses and has already proven its effectiveness in realistic experimental settings [84]. We remark that, even if in the problem at hand the maximum bandwidth is tied to the value of  $M$  (i.e. increasing  $M$  increases the maximum frequency as well), nothing prevents from defining a given frequency interval  $[\omega_{\min}, \omega_{\max}]$  and sampling  $M$  frequencies within it, hence allowing to freely change the number of degrees of freedom in the parametrization without affecting the targeted interval  $[\omega_{\min}, \omega_{\max}]$ .

The extent to which the use of time-dependent control fields can speed up a certain process depends on the control-field strength. For definiteness, in the problem at hand we assume that the control-field strength  $B(t)$  (expressed in units of  $J$ ) during the entire duration of control is within the range  $[-4\pi, 4\pi]$ . To include this con-

straint in our numerical calculations, as the actual figure of merit we employ the target-state infidelity  $1 - \mathcal{F}_{t=T}$  complemented with terms accounting for the penalties incurred when the absolute value of  $B(t)/J$  exceeds  $4\pi$ , i.e.

$$\text{FoM} = 1 - \mathcal{F}_{t=T} + J^{-1} [B_{\max} \Theta(B_{\max}/J - 4\pi) - B_{\min} \Theta(-4\pi - B_{\min}/J)], \quad (26)$$

where  $\Theta(\dots)$  denotes the Heaviside step function, with  $B_{\max} = \max_t B(t)$  and  $B_{\min} = \min_t B(t)$ .

## VI. RESULTS AND DISCUSSION

In the following, we discuss our results obtained for Dicke- and  $W$ -state generation in Heisenberg-coupled arrays with up to  $N = 9$  qubits and a local control field acting in the  $z$  direction on the first qubit in the array. We first present our results for an ideal system [Sec. VI A] and subsequently discuss the effects of control-field distortions from the optimal pulse shape [Sec. VI B], as well as that of control-field leakage away from the actuator qubit [Sec. VI C].

### A. dCRAB-based generation of Dicke states

For every target state, we minimized the figure of merit in Eq. (26) over the parameters  $\{c_m^{(l)}, s_m^{(l)} | m = 0, \dots, M-1; l = 0, \dots, L-1\}$ , for the varying total duration  $T$  of the pulse. In each case, the total evolution time  $T$  is varied in small steps starting from an initial value – for which a high target-state fidelity cannot be achieved – until a high-fidelity realization of the desired target state becomes possible; the shortest time  $T$  for which a realization of the desired state within the assumed fidelity threshold ( $1 - \mathcal{F}_{t=T} < 10^{-3}$ ) is possible is then identified with the shortest possible state-preparation time  $T_{\min}$ .

The results we obtained in the investigated examples of Dicke states, both for the genuine Dicke states ( $a \geq 2$ ) and in the special case of  $W$  states ( $a = 1$ ), are illustrated in Fig. 5. In particular, Fig. 5(a) contains the obtained shortest times  $T_{\min}$  required to realize particular Dicke states; these times are in the range between around  $J^{-1}$  (for the three-qubit  $W$  state) and  $10 J^{-1}$  (for the nine-qubit  $W$  state). At the same time, Fig. 5(b) depicts the target-state infidelities achieved for  $T = T_{\min}$  in the numerical optimization process; as can be inferred from the plot, these infidelities are mostly between  $10^{-3}$  and  $10^{-4}$ .

Our optimal-control approach to engineering Dicke states  $|D_a^N\rangle$  ( $a = 1, \dots, N-1$ ) in an  $N$ -qubit array entails working in a computational basis that consists of  $\binom{N}{a}$  states – the dimension of the  $a$ -excitation subspace  $\mathcal{H}_a$  of the total  $2^N$ -dimensional Hilbert space (recall Sec. IV B above). Given that for the fixed system size  $N$  the dimension of this subspace grows rapidly with increasing

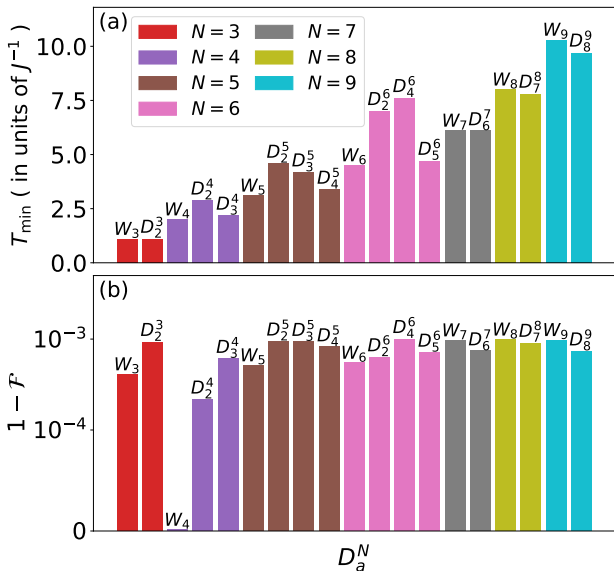


FIG. 5: Pictorial overview of the results obtained using the optimal-control approach based on the dCRAB formalism (with  $M = 15$  harmonics in the truncated random Fourier basis) for an  $N$ -qubit array ( $N = 3, \dots, 9$ ) with isotropic, nearest-neighbor Heisenberg coupling and a  $Z$  control on the first qubit: (a) The shortest times  $T_{\min}$  required for the realization of both genuine Dicke states ( $|D_a^N\rangle$ , with  $a \geq 2$ ) and  $W$  states ( $|W_N\rangle \equiv |D_1^N\rangle$ ); (b) The highest fidelities (i.e. the smallest infidelities  $1 - F$ ) obtained for each of the investigated  $N$ -qubit states through an evolution of duration  $T_{\min}$ .

the excitation number  $a$  – before reaching the maximal value  $N!/([N/2]!)^2$  for  $a = \lfloor N/2 \rfloor$  [which is equal to  $N/2$  for even values of  $N$ , and  $(N-1)/2$  for odd ones] – and, for large  $N$ , even becomes asymptotically exponential in  $N$  [cf. Sec. IV B], the underlying numerical-optimization problem [namely, finding the global minimum of the generalized figure of merit in Eq. (26)] becomes increasingly more demanding from the computational standpoint. As a consequence, the numerical burden involved in engineering Dicke states within our adopted optimal-control scheme becomes computationally prohibitive for large system sizes  $N \gtrsim 10$  and values of  $a$  close to  $N/2$ .

In order to quantitatively assess the potential practical utility of the proposed local-control approach in engineering highly-entangled multiqubit states of Heisenberg-coupled qubit arrays it is of interest to deduce the scaling of the shortest possible state-preparation times  $T_{\min}$  for both  $W$  states and genuine Dicke states with the number of qubits  $N$ . Based on our obtained numerical results, a fitting procedure aimed at extracting a power-law dependence of  $T_{\min}$  on  $N$  yields the result

$$T_{\min}(N) = 0.10 \times N^{2.08} + 0.10 \quad (27)$$

for  $N$ -qubit  $W$  states ( $a = 1$ ), and

$$T_{\min}(N) = 0.34 \times N^{1.78} - 1.25 \quad (28)$$

for Dicke states  $|D_{a=2}^N\rangle$ . Therefore, the scaling of the

shortest possible state-preparation time  $T_{\min}$  obtained using our optimal-control approach based on the dCRAB algorithm with  $N$  is approximately quadratic in  $N$  for  $W$  states and slower than quadratic for  $a = 2$  Dicke states (for an illustration, see Fig. 6). The two curves in Fig. 6 have an intersection for  $N = 3$  because the states  $|D_1^3\rangle \equiv |W_3\rangle$  and  $|D_2^3\rangle$  are equivalent up to the interchange  $|0\rangle \leftrightarrow |1\rangle$  of the single-qubit basis states (recall Sec. II), hence the equal preparation times obtained.

It is pertinent at this point to comment on the obtained dependence of  $T_{\min}$  on  $N$  for Dicke states. It has become well-known by now that an overwhelming majority of the as yet proposed analog schemes for the Dicke-state preparation in various physical systems are characterized by state-preparation times that exhibit superlinear dependence on  $N$  [85, 86]. In this context, our principal finding – the obtained  $\mathcal{O}(N^{1.78})$  scaling of  $T_{\min}(N)$  with  $N$  – represents a rather favorable scaling for an analog Dicke-state preparation scheme. This is especially true given that this last result is obtained by means of what constitutes – from the controllability standpoint – the minimal possible control resource that allows the realization of the sought-after states in an entire class of systems (interacting qubit arrays) – a local  $Z$  control acting on a single actuator qubit. Needless to say, more conventional scenarios of quantum control in interacting qubit arrays in state-of-the-art QC platforms either entail the use of global control fields [18] or time-dependent local control fields acting on each qubit in the array [87].

Generally speaking, the question of obtaining the minimal evolution time of a quantum system subject to external control fields that makes a desired state transformation of the system possible is inextricably linked to the concept of *quantum speed limit* [88]. While the latter concept was originally thought of as that of an in-

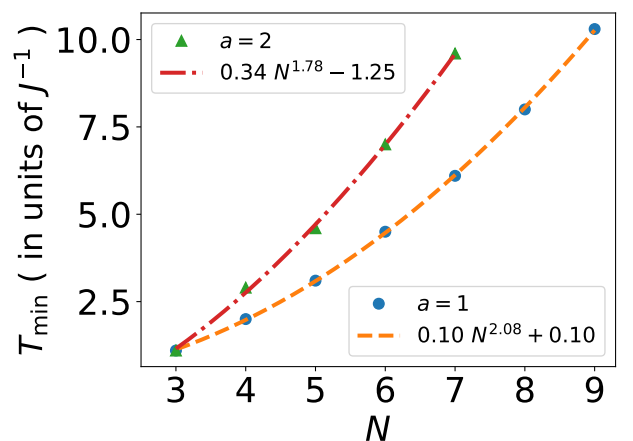


FIG. 6: Illustration of the scaling of the shortest possible state-preparation times, for both  $W$  states  $|W_N\rangle \equiv |D_{a=1}^N\rangle$  and two-excitation Dicke states  $|D_{a=2}^N\rangle$ , with the number  $N$  of qubits. The two scaling laws  $T_{\min}(N)$  are established by fitting the results obtained using the dCRAB formalism, with  $M = 15$  harmonics in the truncated random Fourier basis.

intrinsic timescale of unitary quantum dynamics, subsequent studies explicitly showed the connection between this concept and optimal control [89]. To be more specific, the quantum speed limit was shown to yield the shortest timescale required for quantum optimal-control algorithms to converge; this finding was a *de-facto* demonstration that quantum speed limits are attainable and provided a definition of optimality in the quantum-control context. In the present work, we obtain the shortest times for the generation of highly-entangled Dicke states from an initial product state in accordance with this same criterion of optimality applied in conjunction with the dCRAB algorithm of quantum optimal control. Therefore, the present state-engineering study can be seen as that of generating Dicke states in Heisenberg-coupled qubit arrays with a single local control at the quantum speed limit.

The characteristic time dependencies of optimal control fields  $B_{\text{opt}}(t)$  that enable the realization of Dicke

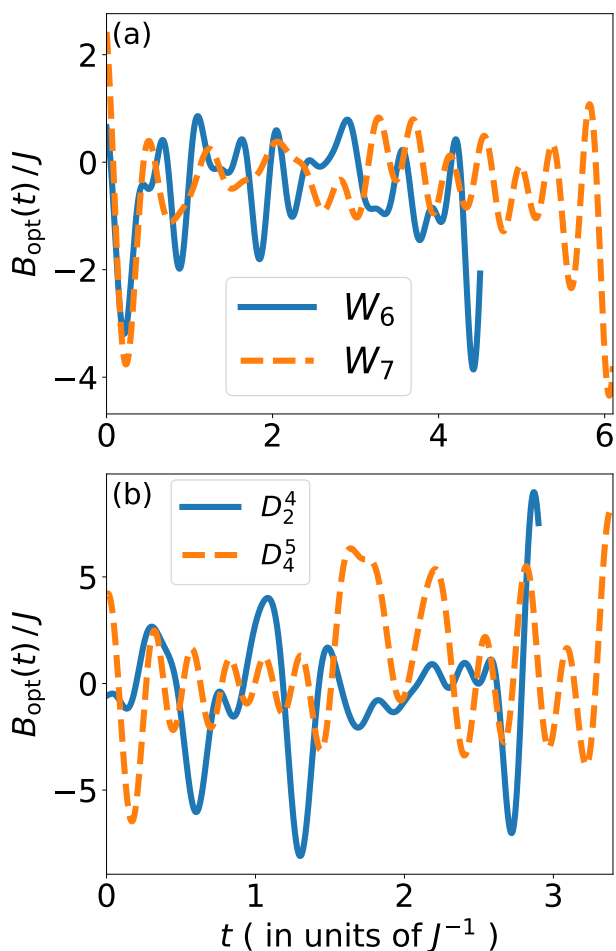


FIG. 7: Optimal control fields  $B_{\text{opt}}(t)$  that enable the realization of (a)  $W$  states  $|W_6\rangle$  and  $|W_7\rangle$ , and (b) Dicke states  $|D_2^4\rangle$  and  $|D_4^5\rangle$ . These results are obtained using the dCRAB formalism, with  $M = 15$  harmonics in the truncated random Fourier basis.

and  $W$  states in the system under consideration are illustrated in Fig. 7. The examples shown correspond to the  $W$  states  $|W_6\rangle, |W_7\rangle$  and Dicke states  $|D_2^4\rangle, |D_4^5\rangle$ ; their corresponding state-preparation times are all in the range between  $2.9J^{-1}$  and  $6.1J^{-1}$ . What is evident from Fig. 7 is that the obtained optimal control fields are varying rapidly with time. It can also be inferred from this plot is that these control-field strengths (expressed in units of  $J$ )  $B_{\text{opt}}(t)/J$  at all times  $0 \leq t \leq T_{\text{min}}$  do not closely approach the upper- and lower bounds of the adopted range  $[-4\pi, 4\pi]$  of values; this underscores the importance of including the penalty terms in the generalized figure of merit FoM [cf. Eq. (26)] that we utilize in this problem and *a posteriori* corroborates the fact that we adopted a sufficiently large range of values of  $B(t)/J$ .

Regarding the practical feasibility of implementing rapidly varying control fields, such as those shown in

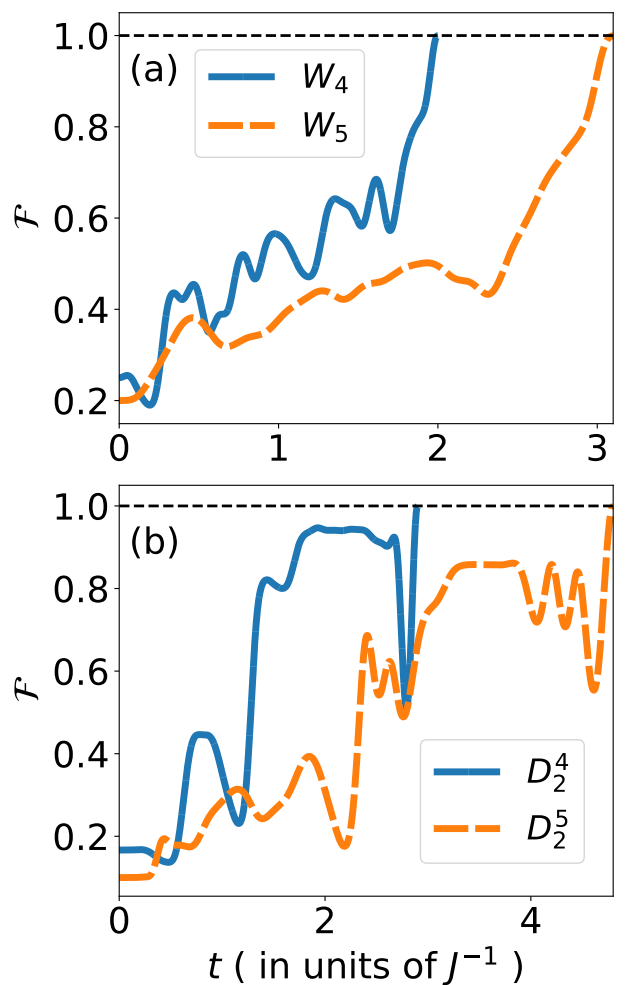


FIG. 8: Time dependence of the target-state fidelity  $\mathcal{F}(t)$  throughout the dynamical evolution that starts from a Hamming-weight- $a$  product state at  $t = 0$  and ends with the Dicke- or  $W$  state at  $t = T_{\text{min}}$ . The examples shown here correspond to (a)  $W$  states  $|W_4\rangle$  and  $|W_5\rangle$ , and (b) Dicke states  $|D_2^4\rangle$  and  $|D_2^5\rangle$ .

Fig. 7, a comment is in order here. In present-day solid-state QC systems (based on superconducting- or spin qubits) operating in the microwave regime [65, 66], shaped control pulses are typically obtained using arbitrary waveform generators (AWGs); such devices are presently available with the clock jitter of 50 ps and sub-nanosecond time resolutions [90]. While in the conventional approach to control-pulse synthesis AWGs only generate a baseband signal and a sought-after pulse is obtained through an upconversion to microwave frequencies by mixing with a carrier, the very high currently achievable sampling rates of AWGs [exceeding 100 gigasamples per second (GSa/s)] combined with analog bandwidths in the tens of GHz (indicating the frequency content that an AWG can reproduce accurately, i.e. without distortions) already allow direct digital synthesis of microwave pulses. This obviates the need for additional microwave generators even in situations where precise waveform shaping is required, i.e. for generating complex custom waveforms.

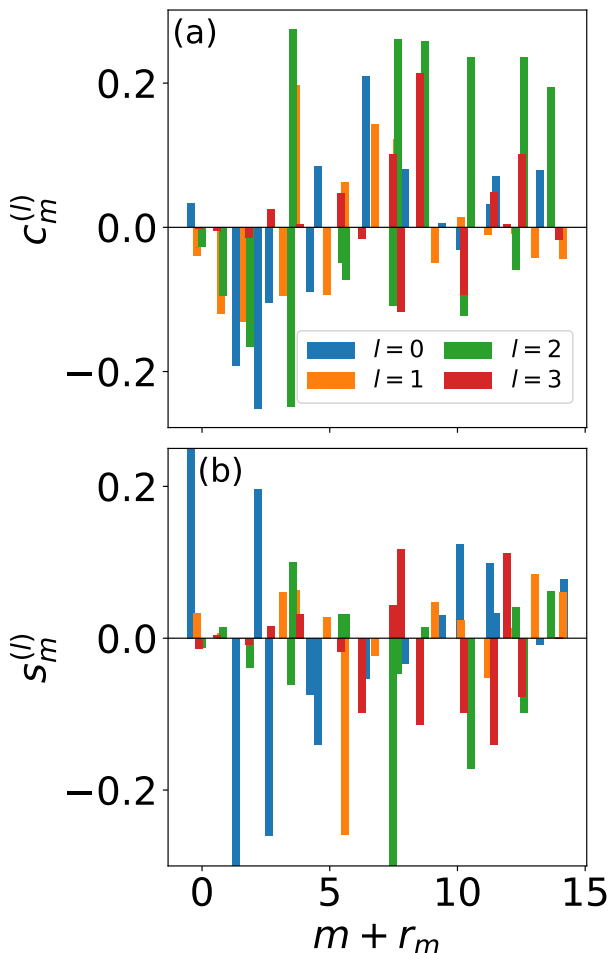


FIG. 9: Optimal parameters (a)  $c_m^{(l)}$ , and (b)  $s_m^{(l)}$ , obtained using the dCRAB formalism. The displayed results correspond to the state  $|W_6\rangle$  and are obtained with  $M = 15$  harmonics in the truncated random Fourier basis. Each color is associated with one specific value of  $l$ , i.e. one specific dressing iteration.

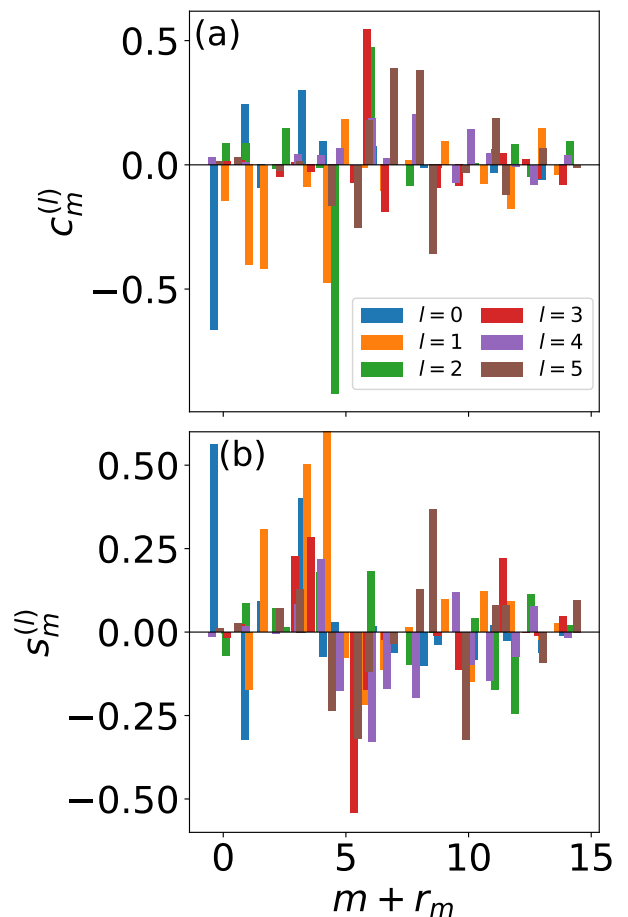


FIG. 10: Optimal parameters (a)  $c_m^{(l)}$ , and (b)  $s_m^{(l)}$ , obtained using the dCRAB formalism. The displayed results correspond to the state  $|D_2^4\rangle$  and are obtained with  $M = 15$  harmonics in the truncated random Fourier basis. Each color is associated with one specific value of  $l$ , i.e. one specific dressing iteration.

Fig. 8 illustrates the time dependence of the state fidelity  $\mathcal{F}(t)$  for both  $W$ - and genuine Dicke states. For the  $a$ -excitation Dicke state  $|D_a^N\rangle$ , the dynamical evolution starts from the Hamming-weight- $a$  product state in Eq. (18); therefore, the initial value of the target-state fidelity is  $\mathcal{F}_{t=0} = \binom{N}{a}^{-1}$ . The fidelity has a rather complex time dependence – this being a consequence of the rapidly-varying control field  $B(t)$  [cf. Fig. 7] – before reaching a value very close to unity at  $t = T_{\min}$ .

In our numerical optimal-control calculations we utilize  $M = 15$  harmonics in the truncated Fourier expansion of Eq. (23). Regarding the dependence of the obtained results on  $M$ , the following remark can be made. It transpires from our numerical calculations that the obtained results depend on  $M$  only in an implicit fashion. To be more specific, a sufficiently large value of  $M$  – i.e. a large enough number of harmonics in the expansion of the control field [cf. Eq. (23)] – is necessary for high-fidelity realizations of Dicke states; in particular, the states  $|D_a^N\rangle$

that correspond to larger values of  $N$  and  $a$  cannot be successfully engineered if  $M$  is too small. However, provided that  $M$  is chosen to be sufficiently large (as is the case for  $M = 15$  that we use in the problem under consideration), the actual minimal state-engineering times for different Dicke states do not show any dependence on  $M$ .

In order to provide a further quantitative characterization of our implementation of the dCRAB formalism, it is instructive to look more closely into the parameters  $c_m^{(l)}$  and  $s_m^{(l)}$  ( $l = 0, \dots, L-1$ ) resulting from the dressing iterations [cf. Sec. V C]. In Figs. 9 and 10 these parameters are displayed for the states  $|W_6\rangle$  and  $|D_2^4\rangle$ , respectively. What can be inferred from these plots is that all dressing iterations [i.e. their corresponding optimization parameters  $c_m^{(l)}$  and  $s_m^{(l)}$  for  $l = 1, \dots, L-1$ ] play an important role in the optimization process, not only the original optimization parameters  $c_m^{(0)} \equiv c_m$  and  $s_m^{(0)} \equiv s_m$  [i.e. coefficients in the original truncated random Fourier expansion of Eq. (25)]. This important conclusion constitutes an *a posteriori* justification for our use of the dCRAB formalism, i.e. our preference for this method rather than its parent CRAB method.

### B. Robustness against control-field distortions from the optimal pulse shape

In quantum-technology applications, in which a high degree of control over the dynamics of quantum systems is often essential, it is crucial to be able to quantify an error resulting from random deviations of an external control field from its optimal values [48, 91]. Therefore, it is usually of pivotal importance to be able to design control pulses which – even if not being optimal – lead to an error in the relevant figure of merit (compared to the optimal value) that is smaller than some predefined threshold value, being at the same time amenable to an experimental realization.

In the Dicke-state engineering problem at hand, we determine the optimal control field  $B_{\text{opt}}(t)$  that permits the realization of a desired Dicke state in the shortest possible time [cf. Sec. VI A]. In accordance with the above general considerations, it is pertinent to quantify the sensitivity of the state-engineering scheme under consideration against deviations from the obtained optimal control fields  $B_{\text{opt}}(t)$ . With this motivation, we consider time-dependent distortions from the optimal control field, which can be parametrized as [91]

$$\delta B(t) = \tau \sin\left(2\pi\kappa \frac{t}{T_{\text{min}}}\right) \frac{d}{dt} B_{\text{opt}}(t), \quad (29)$$

where  $\kappa$  is an integer-valued parameter describing the modulation rate of the optimal pulses; at the same time, the product of  $\tau$ , which has units of time, and the first derivative  $dB_{\text{opt}}(t)/dt$  of the optimal control field constitutes the distortion amplitude. The total distorted

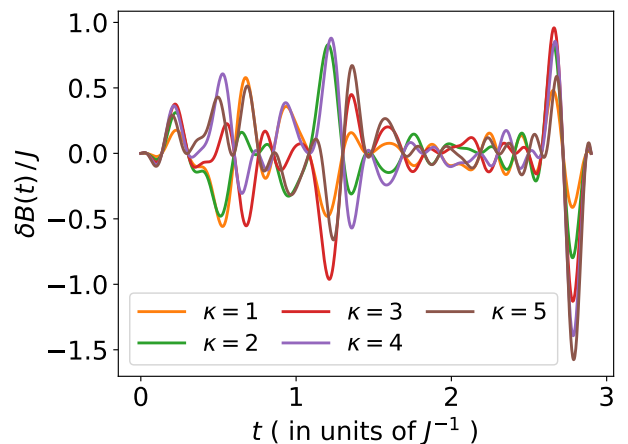


FIG. 11: Illustration of control-field distortions from the optimal control-pulse shape: time-dependence of the control-field distortion  $\delta B(t)$  for  $\tau = 0.01$  and several different values of the parameter  $\kappa$ . The results displayed here correspond to the state  $|D_2^4\rangle$ , realized using the dCRAB formalism with  $M = 15$ ; the optimal control-pulse shape is shown in Fig. 7.

control field corresponding to  $\delta B(t)$  is then given by

$$B_{\text{dist}}(t) \equiv B_{\text{opt}}(t) + \delta B(t). \quad (30)$$

Despite its relatively simple form, the proposed parametrization of control-field distortions suffices to describe – provided that the values of the parameters  $\kappa$  and  $\tau$  are chosen appropriately – an almost arbitrary control-pulse shape [60].

Given the character of optimal control fields  $B_{\text{opt}}(t)$  in the state-engineering problem at hand – which are varying rapidly with time [cf. Fig. 7] – only very small values of the parameter  $\tau$  allow one to mimic small control-pulse distortions characteristic of present-day pulse-shaping hardware [cf. Sec. VI A]. More specifically yet, using the above general expression for time-dependent control-field distortions  $\delta B(t)$  [cf. Eq. (29)], it is straightforward to verify that  $\tau \sim 0.01$  is the appropriate order of magnitude for the value of this parameter that allows one to emulate such small control-pulse distortions. Examples of control-field distortions  $\delta B(t)$  are displayed in Fig. 11 for  $\tau = 0.01$  and several values of the parameter  $\kappa$ .

In the context of the Dicke-state engineering problem at hand, it is of interest to quantify to what extent the presence of small control-field distortions from the optimal pulse shape affects our proposed scheme. To this end, it is necessary to compute the Dicke-state fidelity  $\mathcal{F}_{\text{dist}}$  corresponding to the distorted control field  $B_{\text{dist}}(t)$ , a quantity that can straightforwardly be obtained once the state  $|\psi(t = T_{\text{min}})\rangle$  of the system at  $t = T_{\text{min}}$  is computed. This can be done in a numerically-exact fashion, namely by propagating the time-dependent Schrödinger equation [92] of the system up to  $t = T_{\text{min}}$ . Like in the idealized (distortion-free) case, for the target state  $|D_a^N\rangle$  the initial condition  $|\psi(t = 0)\rangle$  in this last dynamical

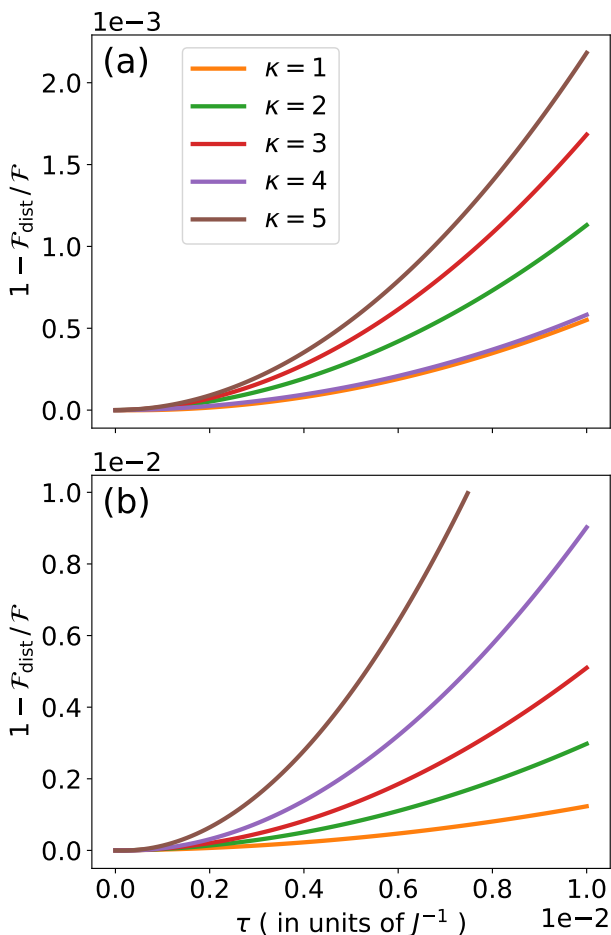


FIG. 12: Relative deviation from the optimal value of the target-state fidelity due to control-field distortions characterized by the parameters  $\tau$  and  $\kappa$ . The results displayed here correspond to the states (a)  $|W_5\rangle$ , and (b)  $|D_2^4\rangle$ , both realized using the dCRAB formalism with  $M = 15$ .

equation is given by the Hamming-weight- $a$  product state in Eq. (18).

An example of the obtained numerical results for the relative deviation  $(\mathcal{F} - \mathcal{F}_{\text{dist}})/\mathcal{F} \equiv 1 - \mathcal{F}_{\text{dist}}/\mathcal{F}$  of the target-state fidelity with respect to its intrinsic (in the absence of control-field distortions) value  $\mathcal{F}$  is displayed in Fig. 12 for a range of values of the parameter  $\tau$  and several different choices of  $\kappa$ . What can be inferred from this plot is that the relative deviation in the state fidelity resulting from the control-field distortions is fairly small; this speaks in favor of the robustness of our state-engineering scheme.

### C. Robustness against control-field leakage away from the actuator qubit

It is important to note that realistic control fields – for instance, magnetic fields realized with the aid of micro-magnets [93] – can never be perfectly localized. In other

words, our assumption about the control field being confined to a single actuator qubit constitutes an idealization. It is thus pertinent to also briefly discuss a more realistic scenario, with a control field that also affects neighboring qubits as a result of control-field leakage. Describing such a scenario requires a slight generalization of our adopted control Hamiltonian  $H_C(t) = B(t)Z_1$ .

Before discussing specific scenarios of control-field leakage, it should be pointed out that leakage effects do not invalidate the rationale behind our use of the local-control approach. Namely, as demonstrated in Ref. 42, the subspace-controllability results remain valid in the presence of leakage. To be more specific, the invariant-subspace structure and controllability of the system remain the same as in the leakage-free case.

Generalized control Hamiltonians, which account for the effects of control-field leakage, can be written in the form [42]

$$H_C^{\text{cl}} = B(t) \sum_{n=1}^N \gamma_n Z_n, \quad (31)$$

where – depending on the specific type (i.e. spatial dependence) of field leakage –  $\gamma_n$  can assume various forms. For the sake of illustration, we consider here two different types of control-field leakage. In the case of exponential control-field leakage away from the actuator qubit  $n_c$  we have  $\gamma_n = e^{-|n-n_c|/\zeta}$ , where  $\zeta$  is the parameter that measures the extent of exponential leakage; note that  $\zeta = 0$  in the idealized (leakage-free) case. Likewise, in the case of Gaussian control-field leakage  $\gamma_n = e^{-(n-n_c)^2/(2\sigma^2)}$ , where  $\sigma$  is the parameter quantifying this type of leakage; once again,  $\sigma = 0$  indicates the complete absence of leakage. In the special  $n_c = 1$  case (i.e. when the first qubit in the array plays the role of the actuator qubit), which is of particular interest here, the above expressions for  $\gamma_n$  go over into  $\gamma_n = e^{-(n-1)/\zeta}$  and  $\gamma_n = e^{-(n-1)^2/(2\sigma^2)}$ , respectively.

In the following, we quantify the effects of control-field leakage in the state-engineering problem at hand by evaluating Dicke-state fidelities in the presence of leakage. In other words, we determine those fidelities with  $B(t) = B_{\text{opt}}(t)$  (i.e. for the optimal control fields computed in the leakage-free case [cf. Sec. VIA]), assuming at the same time that the evolution of the system is governed by the generalized control Hamiltonian of Eq. (31), with  $\gamma_n$  corresponding to either exponential- or Gaussian leakage. To this end, for each desired Dicke (or, in the special case,  $W$ ) state we propagate the corresponding time-dependent Schrödinger equation [92] [with the initial state  $|\psi(t=0)\rangle$  given by Eq. (18) in the case of the target state  $|D_a^N\rangle$ ] up to  $t = T_{\text{min}}$ , i.e. the time corresponding to the time-optimal, dCRAB-based realization of the desired Dicke (or  $W$ ) state [cf. Sec. VIA]. For a range of values of the parameters  $\zeta$  and  $\sigma$  (for exponential- and Gaussian leakage, respectively), we then compute the fidelity  $\mathcal{F}_{\text{leak}}$  as the module squared of the overlap between the target Dicke (or  $W$ ) state and the

actual state  $|\psi_{\text{leak}}(t = T_{\text{min}})\rangle$  of the system at  $t = T_{\text{min}}$  in the presence of leakage, obtained as described above.

We choose the range  $[0, 0.5]$  of values for the parameters  $\zeta$  and  $\sigma$ . In particular, for the largest considered value  $\zeta = \sigma = 0.5$  of those parameters, the control-field leakage on the nearest neighbor ( $n = 2$ ) of the actuator qubit amounts – for both exponential- and Gaussian control-field leakage – to  $e^{-2} \approx 13.5\%$  of the control-field magnitude on the actuator qubit. On the other hand, for their median value  $\zeta = \sigma = 0.25$ , one has  $e^{-4} \approx 1.8\%$  of the original magnitude in the exponential- and  $e^{-8} \approx 0.03\%$  in the Gaussian-leakage case.

The effect of control-field leakage on the  $W$ - and Dicke-state fidelities – as quantified by the relative deviation  $(\mathcal{F} - \mathcal{F}_{\text{leak}})/\mathcal{F} \equiv 1 - \mathcal{F}_{\text{leak}}/\mathcal{F}$  of the target-state fidelity with respect to its intrinsic (in the absence of leakage) value  $\mathcal{F}$  – is illustrated in Fig. 13 for both exponential- and Gaussian leakage. What can be inferred from the

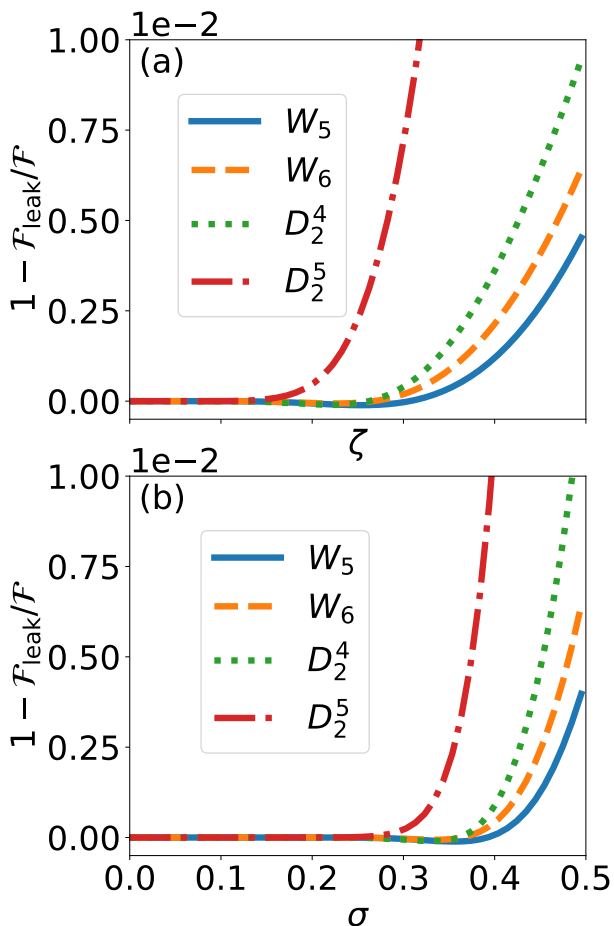


FIG. 13: Relative deviations  $1 - \mathcal{F}_{\text{leak}}/\mathcal{F}$  of the Dicke- and  $W$  state fidelities  $\mathcal{F}_{\text{leak}}$  in the presence of control-field leakage away from the actuator qubit from their intrinsic optimal values  $\mathcal{F}$  obtained using the dCRAB formalism with  $M = 15$ . The results shown here correspond to the cases of (a) exponential leakage, described by the parameter  $\zeta$ , and (b) Gaussian leakage, described by the parameter  $\sigma$ .

obtained results is that the dependence of  $1 - \mathcal{F}_{\text{leak}}/\mathcal{F}$  on  $\zeta$  (or  $\sigma$ ) is very similar for all target states considered. In addition, an important quantitative conclusion can also be drawn from Fig. 13; namely, for a reasonable range of values of parameters  $\zeta$  and  $\sigma$ , the resulting fidelities in the presence of leakage ( $\mathcal{F}_{\text{leak}}$ ) are reduced from the corresponding intrinsic values ( $\mathcal{F}$ ) by an amount of the order of  $10^{-3}$ , i.e. 0.1%. This finding convincingly demonstrates the robustness of our optimal local-control scheme for Dicke-state generation against control-field leakage away from the actuator qubit.

## VII. SUMMARY AND CONCLUSIONS

In summary, the feasibility of time-efficient analog (single-shot) realizations of Dicke states was investigated in this paper for qubit arrays with the isotropic, nearest-neighbor Heisenberg coupling between qubits and a single Zeeman-type local (i.e. acting on a single actuator qubit) control in the  $z$  direction. The theoretical underpinning for the state-control scheme that permits engineering of Dicke states  $|D_a^N\rangle$  starting from a generic Hamming-weight- $a$  product state is provided by an already proven, general result in the realm of Lie-algebraic controllability of interacting spin-1/2 chains (qubit arrays). This result guarantees the subspace controllability of Heisenberg-coupled qubit arrays on any subspace of the total  $N$ -qubit Hilbert space that is characterized by a fixed number of excitations (i.e. a fixed Hamming weight). More specifically yet, this result implies – if a  $Z$  control is applied to a single qubit – that a time-dependent control field can be found that allows one to realize the Dicke state with the desired excitation number  $a$  starting from an arbitrary product state with the same number of excitations.

The problem of finding the appropriate time-dependence of the control field acting on an actuator qubit for engineering Dicke states – including  $W$  states as their special, single-excitation case – in the shortest possible time was addressed here for linear arrays with up to 9 qubits using methods of quantum optimal control. More specifically yet, the search for optimal, smoothly-varying control fields that enable the realization of both  $W$ - and genuine Dicke states at the quantum speed limit was carried out using the dCRAB algorithm, which we implemented in combination with advanced methods of global optimization. In particular, based on our obtained numerical results, we showed that the shortest possible times required for high-fidelity realizations of  $W$  states and  $a = 2$  Dicke states in a Heisenberg-coupled  $N$ -qubit array in this single-control setting scale as  $\mathcal{O}(N^{2.08})$  and  $\mathcal{O}(N^{1.78})$ , respectively. To demonstrate the practical viability of our proposed state-engineering scheme, its sensitivity to imperfections – such as control-field distortions from the optimal pulse shape and control-field leakage away from the actuator qubit – was also investigated, yielding favorable results.

To conclude, the present work underscores the potential usefulness of optimal-control schemes for engineering robust highly-entangled multiqubit states of interest for quantum-technology applications. In addition, it points to the utility of the local-control approach – i.e. the use

of minimal control resources that permit the realization of a desired quantum-control task – in this context. Experimental realizations of such approaches, especially in the context of solid-state qubits, are clearly called for.

- 
- [1] R. H. Dicke, Coherence in Spontaneous Radiation Processes, *Phys. Rev.* **93**, 99 (1954).
- [2] M. Bergmann and O. Gühne, J. Entanglement criteria for Dicke states, *Phys. A: Math. Theor.* **46**, 385304 (2013).
- [3] A. Neven, J. Martin, and T. Bastin, Entanglement robustness against particle loss in multiqubit systems, *Phys. Rev. A* **98**, 062335 (2018).
- [4] W. Zhang, Z. Han, F. Shi, and X. Zhang, Constructions of multipartite entanglement resistant to particle loss, *Phys. Rev. A* **112**, 022408 (2025).
- [5] D. A. Lidar and K. B. Whaley, Decoherence-Free Subspaces and Subsystems, in *Irreversible Quantum Dynamics* (Springer, Berlin Heidelberg, 2003), pp. 83-120.
- [6] V. M. Stojanović and J. K. Nauth, Dicke-state preparation through global transverse control of Ising-coupled qubits, *Phys. Rev. A* **108**, 012608 (2023).
- [7] S. K. Özdemir, J. Shimamura, and N. Imoto, A necessary and sufficient condition to play games in quantum mechanical settings, *New J. Phys.* **9**, 43 (2007).
- [8] R. Prevedel, G. Cronenberg, M. S. Tame, M. Paternostro, P. Walther, M. S. Kim, and A. Zeilinger, Experimental Realization of Dicke States of up to Six Qubits for Multiparty Quantum Networking, *Phys. Rev. Lett.* **103**, 020503 (2009).
- [9] G. Toth, Multipartite entanglement and high-precision metrology, *Phys. Rev. A* **85**, 022322 (2012).
- [10] Z. H. Saleem, M. Perlin, A. Shaji, and S. K. Gray, Achieving the Heisenberg limit with Dicke states in noisy quantum metrology, *Phys. Rev. A* **109**, 052615 (2024).
- [11] See, e.g., Y. Ouyang, Permutation-invariant quantum codes, *Phys. Rev. A* **90**, 062317 (2014).
- [12] See, e.g., J. Golden, A. Bärttschi, D. O'Malley, and S. Eidenbenz, Threshold-Based Quantum Optimization, *Proc. IEEE Int. Conf. Quantum Comput. Eng.*, pp. 137 (2021).
- [13] D. B. Hume, C. W. Chou, T. Rosenband, and D. J. Wineland, Preparation of Dicke states in an ion chain, *Phys. Rev. A* **80**, 052302 (2009).
- [14] L. Lamata, C. E. López, B. P. Lanyon, T. Bastin, J. C. Retamal, and E. Solano, Deterministic generation of arbitrary symmetric states and entanglement classes, *Phys. Rev. A* **87**, 032325 (2013).
- [15] J. K. Stockton, R. van Handel, and H. Mabuchi, Deterministic Dicke-state preparation with continuous measurement and control, *Phys. Rev. A* **70**, 022106 (2004).
- [16] Y.-F. Xiao, X.-B. Zou, and G.-C. Guo, Generation of atomic entangled states with selective resonant interaction in cavity quantum electrodynamics, *Phys. Rev. A* **75**, 012310 (2007).
- [17] X.-Q. Shao, L. Chen, S. Zhang, Y.-F. Zhao, and K.-H. Yeon, Deterministic generation of arbitrary multi-atom symmetric Dicke states by a combination of quantum Zeno dynamics and adiabatic passage, *EPL* **90**, 50003 (2010).
- [18] A. Muratori, V. M. Stojanović, E. Cuestas, T. Calarco, and F. Motzoi, *W*- and Dicke-state engineering using optimal global control in nearest-neighbor coupled ring-shaped qubit arrays, arXiv:2512.19545.
- [19] C.-y. Zhang and J. Jing, Efficient nonclassical state preparation via generalized parity measurement, *Phys. Rev. A* **113**, 022420 (2026).
- [20] W. Wieczorek, R. Krischek, N. Kiesel, P. Michelberger, G. Toth, and H. Weinfurter, Experimental Entanglement of a Six-Photon Symmetric Dicke State, *Phys. Rev. Lett.* **103**, 020504 (2009).
- [21] C. Wu, C. Guo, Y. Wang, G. Wang, X.-L. Feng, and J.-L. Chen, Generation of Dicke states in the ultrastrong-coupling regime of circuit QED systems, *Phys. Rev. A* **95**, 013845 (2017).
- [22] T. Kobayashi, R. Ikuta, Ş. Kaya Özdemir, M. Tame, T. Yamamoto, M. Koashi, and N. Imoto, Universal gates for transforming multipartite entangled Dicke states, *New J. Phys.* **16**, 023005 (2014).
- [23] F. Albarran-Arriagada, G. Romero, and J. C. Retamal, Equally entangled multiqubit states, *Phys. Scr.* **101**, 115102 (2026).
- [24] V. Jurdjević and H. J. Sussmann, Control systems on Lie groups, *J. Differ. Equations* **12**, 313 (1972).
- [25] G. M. Huang, T. J. Tarn, and J. W. Clark, On the controllability of quantum-mechanical systems, *J. Math. Phys.* **24**, 2608 (1983).
- [26] V. Ramakrishna and H. Rabitz, Relation between quantum computing and quantum controllability, *Phys. Rev. A* **54**, 1715 (1996).
- [27] D. D'Alessandro, *Introduction to Quantum Control and Dynamics* (Taylor & Francis, Boca Raton, 2008).
- [28] C. P. Koch, U. Boscain, T. Calarco, G. Dirr, S. Filipp, S. J. Glaser, R. Kosloff, S. Montangero, T. Schulte-Herbrüggen, D. Sugny, and F. K. Wilhelm, Quantum control for advanced technology: Past and present, *EPJ Quantum Tech.* **9**, 19 (2022).
- [29] M. M. Müller, R. S. Said, F. Jelezko, T. Calarco, and S. Montangero, One decade of quantum optimal control in the chopped random basis, *Rep. Prog. Phys.* **85**, 076001 (2022).
- [30] Q. Ansel, E. Dionis, F. Arrouas, B. Peaudecerf, S. Guerin, D. Guery-Odelin, and D. Sugny, Introduction to theoretical and experimental aspects of quantum optimal control, *J. Phys. B: At. Mol. Opt. Phys.* **57**, 133001 (2024).
- [31] For a recent review, see C. W. Duncan, P. M. Poggi, M. Bukov, N. T. Zinner, and S. Campbell, Taming Quantum Systems: A Tutorial for Using Shortcuts-To-Adiabaticity, Quantum Optimal Control, and Reinforcement Learning, *PRX Quantum* **6**, 040201 (2025).
- [32] P. Cappellaro, C. Ramanathan, and D. G. Cory, Dynamics and Control of a Quasi-1D Spin System, *Phys. Rev. Lett.* **99**, 250506 (2007).

- [33] L. Stefanescu, L. Edwards-Pratt, J. O'Connor, E. Tsegaye, N. H. Le, and F. Mintert, Robust implicit quantum control of interacting spin chains, *Phys. Rev. A* **112**, 012609 (2025).
- [34] A. L. P. de Lima, J.-S. Li, L. S. Baker, A. Zlotnik, A. K. Harter, and M. J. Martin, Robust Quantum State Generation in Symmetric Spin Networks, arXiv:2511.01085.
- [35] D. P. DiVincenzo, D. Bacon, J. Kempe, G. Burkard, and K. B. Whaley, Universal quantum computation with the exchange interaction, *Nature (London)* **408**, 339 (2000).
- [36] M. A. Nielsen and I. L. Chuang, *Quantum Computation and Quantum Information* (Cambridge University Press, Cambridge, 2000).
- [37] J. Levy, Universal Quantum Computation with Spin-1/2 Pairs and Heisenberg Exchange, *Phys. Rev. Lett.* **89**, 147902 (2002).
- [38] D. Bacon, J. Kempe, D. A. Lidar, and K. B. Whaley, Universal Fault-Tolerant Quantum Computation on Decoherence-Free Subspaces, *Phys. Rev. Lett.* **85**, 1758 (2000).
- [39] T. Tanamoto, D. Becker, V. M. Stojanović, and C. Bruder, Preserving universal resources for one-way quantum computing, *Phys. Rev. A* **86**, 032327 (2012).
- [40] See, e.g., T. Tanamoto, V. M. Stojanović, C. Bruder, and D. Becker, Strategy for implementing stabilizer-based codes on solid-state qubits, *Phys. Rev. A* **87**, 052305 (2013).
- [41] S. G. Schirmer, I. C. H. Pullen, and P. J. Pemberton-Ross, Global controllability with a single local actuator, *Phys. Rev. A* **78**, 062339 (2008).
- [42] X. Wang, D. Burgarth, and S. Schirmer, Subspace controllability of spin-1/2 chains with symmetries, *Phys. Rev. A* **94**, 052319 (2016).
- [43] S. C. Benjamin and S. Bose, Quantum Computing with an Always-On Heisenberg Interaction, *Phys. Rev. Lett.* **90**, 247901 (2003).
- [44] R. Heule, C. Bruder, D. Burgarth, and V. M. Stojanović, Local quantum control of Heisenberg spin chains, *Phys. Rev. A* **82**, 052333 (2010).
- [45] Z. Zimboras, R. Zeier, T. Schulte-Herbrüggen, and D. Burgarth, Symmetry criteria for quantum simulability of effective interactions, *Phys. Rev. A* **92**, 042309 (2015).
- [46] F. Albertini and D. D'Alessandro, Quantum subspace controllability implying full controllability, *Linear Algebra Appl.* **705**, 207 (2025).
- [47] R. Heule, C. Bruder, D. Burgarth, and V. M. Stojanović, Controlling qubit arrays with anisotropic XXZ Heisenberg interaction by acting on a single qubit, *Eur. Phys. J. D* **63**, 41 (2011).
- [48] V. M. Stojanović, Feasibility of single-shot realizations of conditional three-qubit gates in exchange-coupled qubit arrays with local control, *Phys. Rev. A* **99**, 012345 (2019).
- [49] T. J. Green, J. Sastrawan, H. Uys, and M. J. Biercuk, Arbitrary quantum control of qubits in the presence of universal noise, *New J. Phys.* **15**, 095004 (2013).
- [50] W. H. Press, S. A. Teukolsky, W. T. Vetterling, and B. P. Flannery, *Numerical Recipes in C: The Art of Scientific Computing* (Cambridge University Press, Cambridge, 1999).
- [51] A. Törn and A. Žilinskas, *Global Optimization*, Lecture Notes in Computer Science, vol 350 (Springer, Berlin, 1989).
- [52] V. M. Stojanović, Bare-Excitation Ground State of a Spinless-Fermion-Boson Model and  $W$ -State Engineering in an Array of Superconducting Qubits and Resonators, *Phys. Rev. Lett.* **124**, 190504 (2020).
- [53] V. M. Stojanović, Scalable  $W$ -type entanglement resource in neutral-atom arrays with Rydberg-dressed resonant dipole-dipole interaction, *Phys. Rev. A* **103**, 022410 (2021).
- [54] J. Zheng, J. Peng, P. Tang, F. Li, and N. Tan, Unified generation and fast emission of arbitrary single-photon multimode  $W$  states, *Phys. Rev. A* **105**, 062408 (2022).
- [55] G. Q. Zhang, W. Feng, W. Xiong, Q. P. Su, and C. P. Yang, Generation of long-lived  $W$  states via reservoir engineering in dissipatively coupled systems, *Phys. Rev. A* **107**, 012410 (2023).
- [56] V. M. Stojanović and J. K. Nauth, Interconversion of  $W$  and Greenberger-Horne-Zeilinger states for Ising-coupled qubits with transverse global control, *Phys. Rev. A* **106**, 052613 (2022).
- [57] E. Lötstedt and K. Yamanouchi, Comparison of encoding schemes for quantum computing of  $S > 1/2$  spin chains, *Phys. Rev. A* **111**, 062416 (2025).
- [58] T. Haase, G. Alber, and V. M. Stojanović, Conversion from  $W$  to Greenberger-Horne-Zeilinger states in the Rydberg-blockade regime of neutral-atom systems: Dynamical-symmetry-based approach, *Phys. Rev. A* **103**, 032427 (2021).
- [59] T. Haase, G. Alber, and V. M. Stojanović, Dynamical generation of chiral  $W$  and Greenberger-Horne-Zeilinger states in laser-controlled Rydberg-atom trimers, *Phys. Rev. Res.* **4**, 033087 (2022).
- [60] J. K. Nauth and V. M. Stojanović, Quantum-brachistochrone approach to the conversion from  $W$  to Greenberger-Horne-Zeilinger states for Rydberg-atom qubits, *Phys. Rev. A* **106**, 032605 (2022).
- [61] H. Sharma and U. T. Bhosale, Exact solvability of entanglement for arbitrary initial state in an infinite-range Floquet system, *Ann. Phys. (N.Y.)* **486**, 170327 (2026).
- [62] W. Pfeifer, *The Lie Algebras  $su(N)$ : An Introduction* (Birkhäuser, Basel, 2003).
- [63] See, e.g., S. Lorenzo, T. J. G. Apollaro, A. Sindona, and F. Plastina, Quantum-state transfer via resonant tunneling through local-field-induced barriers, *Phys. Rev. A* **87**, 042313 (2013).
- [64] M. Veldhorst, H. G. J. Eenink, C. H. Yang, and A. S. Dzurak, Silicon CMOS architecture for a spin-based quantum computer, *Nat. Commun.* **8**, 1766 (2017).
- [65] See, e.g., I. Hansen, A. E. Seedhouse, A. Saraiva, A. Laucht, A. S. Dzurak, and C. H. Yang, Pulse engineering of a global field for robust and universal quantum computation, *Phys. Rev. A* **104**, 062415 (2021).
- [66] H. C. George, M. T. Madzik, E. M. Henry, A. J. Wagner, M. M. Islam, F. Borjans, E. J. Connors, J. Corrigan, M. Curry, M. K. Harper, *et al.*, 12-Spin-Qubit Arrays Fabricated on a 300 mm Semiconductor Manufacturing Line, *Nano Lett.* **25**, 793 (2025).
- [67] R. Aiudi, J. Despres, R. Menta, A. Abedi, G. Menichetti, V. Giovannetti, M. Polini, and F. Caravelli, Overcoming disorder in superconducting globally driven quantum computing, *Phys. Rev. A* **113**, 012616 (2026).
- [68] J. Preskill, Quantum Computing in the NISQ era and beyond, *Quantum* **2**, 79 (2018).
- [69] J. Chen, Y. Zhou, J. Bian, J. Li, and X. Peng, Subspace controllability of symmetric spin networks, *Phys. Rev. A* **102**, 032602 (2020).

- [70] V. Evangelakos, E. Paspalakis, and D. Stefanatos, Fast charging of an Ising-spin-pair quantum battery using optimal control, *Phys. Rev. A* **110**, 052601 (2024).
- [71] D. Koutromanos, D. Stefanatos, and E. Paspalakis, Fast generation of entanglement between coupled spins using optimization and deep learning methods, *EPJ Quantum Technol.* **11**, 85 (2024).
- [72] V. Evangelakos, E. Paspalakis, and D. Stefanatos, Fast protocols for charging a three-spin-chain quantum battery, *Sci. Rep.* **15**, 45626 (2025).
- [73] H. Zhou, Q. Hu, Y. Chen, T. Wang, F. Jin, Y. Ji, J. Geng, and X. Peng, Fast conversion from  $W$  to Greenberger-Horne-Zeilinger states via inverse engineering, *Phys. Rev. Appl.* **25**, 014056 (2026).
- [74] See, e.g., S. S. Ivanov, P. A. Ivanov, I. E. Linington, and N. V. Vitanov, Scalable quantum search using trapped ions, *Phys. Rev. A* **81**, 042328 (2010).
- [75] V. M. Stojanović, A. Fedorov, A. Wallraff, and C. Bruder, Quantum-control approach to realizing a Toffoli gate in circuit QED, *Phys. Rev. B* **85**, 054504 (2012).
- [76] N. Khaneja, T. Reiss, C. Kehlet, T. Schulte-Herbrüggen, and S. J. Glaser, Optimal control of coupled spin dynamics: design of NMR pulse sequences by gradient ascent algorithms, *J. Magn. Reson.* **172**, 296 (2005).
- [77] M. H. Goerz, D. Basilewitsch, F. Gago-Encinas, M. G. Krauss, K. P. Horn, D. M. Reich, and C. Koch, Krotov: A Python implementation of Krotov's method for quantum optimal control, *SciPost Phys.* **7**, 080 (2019).
- [78] T. Caneva, T. Calarco, and S. Montangero, Chopped random-basis quantum optimization, *Phys. Rev. A* **84**, 022326 (2011).
- [79] N. Rach, M. M. Müller, T. Calarco, and S. Montangero, Dressing the chopped-random-basis optimization: A bandwidth-limited access to the trap-free landscape, *Phys. Rev. A* **92**, 062343 (2015).
- [80] D. Lucarelli, Quantum optimal control via gradient ascent in function space and the time-bandwidth quantum speed limit, *Phys. Rev. A* **97**, 062346 (2018).
- [81] D. Lewis, R. Wiersema, and S. Bose, Quantum Optimal Control with Geodesic Pulse Engineering, arXiv:2508.16029.
- [82] V. M. Stojanović and M. Vanević, Quantum-entanglement aspects of polaron systems, *Phys. Rev. B* **78**, 214301 (2008).
- [83] See, e.g., V. M. Stojanović, Entanglement-spectrum characterization of ground-state nonanalyticities in coupled excitation-phonon models, *Phys. Rev. B* **101**, 134301 (2020).
- [84] A. Omran, H. Levine, A. Keesling, G. Semeghini, T. T. Wang, S. Ebadi, H. Bernien, A. S. Zibrov, H. Pichler, S. Choi, *et al.*, Generation and manipulation of Schrödinger cat states in Rydberg atom arrays, *Science* **365**, 570 (2019).
- [85] T. Keating, C. H. Baldwin, Y.-Y. Jau, J. Lee, G. W. Biedermann, and I. H. Deutsch, Arbitrary Dicke-State Control of Symmetric Rydberg Ensembles, *Phys. Rev. Lett.* **117**, 213601 (2016).
- [86] M. T. Johnsson, N. R. Mukty, D. Burgarth, T. Volz, and G. K. Brennen, Geometric Pathway to Scalable Quantum Sensing, *Phys. Rev. Lett.* **125**, 190403 (2020).
- [87] C. Arenz and H. Rabitz, Controlling Qubit Networks in Polynomial Time, *Phys. Rev. Lett.* **120**, 220503 (2018).
- [88] For a review, see S. Deffner and S. Campbell, Quantum speed limits: from Heisenberg's uncertainty principle to optimal quantum control, *J. Phys. A: Math. Theor.* **50**, 453001 (2017).
- [89] T. Caneva, M. Murphy, T. Calarco, R. Fazio, S. Montangero, V. Giovannetti, and G. E. Santoro, Optimal Control at the Quantum Speed Limit, *Phys. Rev. Lett.* **103**, 240501 (2009).
- [90] Hd AWG specifications, Zurich Instruments report (2020).
- [91] A. Negretti, R. Fazio, and T. Calarco, Errors in quantum optimal control and strategy for the search of easily implementable control pulses, *J. Phys. B* **44**, 154012 (2011).
- [92] V. M. Stojanović and I. Salom, Quantum dynamics of the small-polaron formation in a superconducting analog simulator, *Phys. Rev. B* **99**, 134308 (2019).
- [93] M. Pioro-Ladriere, T. Obata, Y. Tokura, Y.-S. Shin, T. Kubo, K. Yoshida, T. Taniyama, and S. Tarucha, Electrically driven single-electron spin resonance in a slanting Zeeman field, *Nat. Phys.* **4**, 776 (2008).